Eur. J. Mineral., 35, 439–459, 2023
https://doi.org/10.5194/ejm-35-439-2023


European Journal of Mineralogy
Open Access

# Mineralogy and mineral chemistry of detrital platinum-group minerals and gold particles from the Elbe, Germany

**Malte Junge**[1,2], **Simon Goldmann**[3], **and Hermann Wotruba**[4,†]

[1]Mineralogical State Collection Munich, MSM-SNSB, Theresienstraße 41, 80333 Munich, Germany
[2]Department für Geo- und Umweltwissenschaften/Department of Earth and Environmental Sciences, Ludwig Maximilian University of Munich, Theresienstraße 41, 80333 Munich, Germany
[3]Natural Resources, Federal Institute for Geosciences and Natural Resources (BGR), Stilleweg 2, 30655 Hanover, Germany
[4]Mineral Processing Unit (AMR), RWTH Aachen University, Lochnerstraße 4–20, 52064 Aachen, Germany
†deceased

**Correspondence:** Malte Junge (malte.junge@lrz.uni-muenchen.de)

Received: 8 February 2023 – Revised: 26 May 2023 – Accepted: 6 June 2023 – Published: 6 July 2023

**Abstract.** In heavy mineral concentrates of the Elbe, gold and platinum-group minerals (PGMs) are observed. Two fractions ($> 63$ and $< 63\,\mu m$) of the concentrate are analyzed by reflected-light microscopy, scanning electron microscopy with automated mineralogy software and electron microprobe analysis (EPMA). Other heavy minerals are cassiterite, ferberite, monazite, uraninite, columbite–tantalite, magnetite, zircon and cinnabar. Scanning electron microscopy determined the modal abundance of PGMs, gold and the other heavy minerals. The PGMs are mainly Os–Ir–Ru–(Pt) alloys, Pt–Fe alloys, sperrylite and rustenburgite. Compositional variation of PGMs and gold was analyzed by EPMA. This showed that Pt–Fe alloys are (1) native platinum ($> 80$ atom %), (2) ferroan Pt (20 atom % to 50 atom % Fe), (3) isoferroplatinum (2.64 to 3.04 apfu of sum PGE, platinum-group element), (4) tetraferroplatinum group with $Ni + Cu + Fe \approx 50$ atom %, and (5) $\gamma$(Pt,Fe) with sum PGE $> 3.04$ apfu. The Os–Ir–Ru–(Pt) alloys show large compositional variations. Platinum and Fe enrichment is typically observed for Ir-rich Os–Ir–Ru alloys. Gold particles often show compositional zoning of Ag-rich cores and Ag-poor rims due to selective leaching of Ag. Similarly, Hg-rich rims of gold particles are analyzed. These are interpreted as the results of in situ amalgamation due to mobilization of Hg from the associated cinnabar particles. The size and shape of the gold particles generally argue for short transportation distances. Similarly, almost euhedral sperrylite and Pt–Fe alloys suggest a source region close to the sampling site. However, roundish Os–Ir–Ru–(Pt) alloys presumably have experienced longer transportation in the river. Gabbroic dikes of the Lusatia block contain sperrylite and gold particles, which can be the source for these particles found in the concentrate. The composition of the Os–Ir–Ru–(Pt) alloys is similar to previous studies on the Vestřev placer in Czech Republic. Both locations are within the drainage area of the Elbe and can therefore be the source of the PGM and gold particles in the concentrate.

**Published by Copernicus Publications on behalf of the European mineralogical societies DMG, SEM, SIMP & SFMC.**

## 1 Introduction

Major raw materials within the Elbe are gravel and sand, which are mined for the construction industry. However, these gravels and sands contain enrichments of heavy minerals. Heavy mineral concentrates in rivers generally include cassiterite, ferberite, monazite, uraninite, columbite–tantalite, magnetite, zircon and garnet, as well as platinum-group minerals (PGMs) and gold (Dill, 2007; Dill et al., 2009; Hallbauer and Utter, 1977; Oberthür et al., 2016; Slingerland, 1984; Vital et al., 1999; Wierchowiec, 2007). Historically, placer deposits were the only source for platinum-group elements (PGEs) until the discovery of the major ore bodies of the Bushveld Complex in South Africa, the Great Dyke in Zimbabwe, Norilsk in Russia and Sudbury in Canada. In these placers, PGEs occur as discrete mineral phases forming a large group of PGMs, which mainly consists of PGE alloys accompanied by minor amounts of PGE arsenides, sulfides, sulfarsenides, bismuthides and tellurides (Cabri, 2002; Cabri et al., 1996; Oberthür, 2018; Weiser, 2002). The PGE alloys consist mainly of two different groups, i.e., Pt–Fe alloys and Os–Ir–Ru alloys. The nomenclature of Os–Ir–Ru alloys is used and generally accepted according to Harris and Cabri (1991). A revised Pt–Fe phase diagram was recently presented (Cabri et al., 2022b) to update the one by Cabri and Feather (1975).

In general more than 90 % of PGMs in placers are alloys of Pt–Fe and Os–Ir–Ru–Pt with wide ranges of compositions, whereas PGE sulfides are rare (Cabri et al., 2022a; Weiser, 2002). The PGMs in placers can typically be traced to the source region (e.g., ophiolites, Uralian–Alaskan-type complexes or layered intrusions) by their characteristic compositions (Cabri et al., 1996, 2022a; Garuti et al., 1997; Weiser, 2002). For example, Os–Ir–Ru alloys (Os > Ru > Ir > Pt) mainly occur in ophiolites (Cabri et al., 1996, 2022a; González-Jiménez et al., 2009; Weiser, 2002), whereas Pt–Fe alloys usually originate from Uralian–Alaskan-type complexes (Cabri et al., 2022a, b; Cabri and Genkin, 1991; Rudashevsky et al., 2002; Tolstykh et al., 2004; Weiser, 2002; Zaccarini et al., 2018), and layered intrusions host a large variety of PGE sulfides and arsenides such as laurite, cooperite–braggite and sperrylite, as well as PGE bismuthotellurides and other rare PGM. However, Os–Ir–Ru alloys from layered intrusions are scarce (Cabri et al., 2022a; Junge et al., 2014; Oberthür, 2011, 2018; Oberthür et al., 2014, 2016; Weiser, 2002). In ophiolites, Pt–Fe alloys exist, but these are rare and characterized by high Fe, Cu and Ni contents (Cabri et al., 2022a; Weiser, 2002). Recently, it was shown that PGMs rich in Pt, Pd and Rh (relative to Ru, Os and Ir) exist in ophiolites associated with sulfide-bearing chromitites (González-Jiménez et al., 2014a, b; O'Driscoll and González-Jiménez, 2015; Prichard and Brought, 2009; Zaccarini et al., 2022).

Generally, PGMs are primary and are formed by magmatic or post-magmatic processes. These primary PGMs were subsequently liberated from the host rock by weathering and transported by physical processes (Barkov and Cabri, 2019; Cabri et al., 1996, 2022a; Cabri and Harris, 1975; Oberthür, 2018). In primary PGE ores, nanometer-sized particles of Pt–Fe–Cu alloys were found that formed by coalescence of clusters (Junge et al., 2015; Pushkarev et al., 2018). These nanometer-sized clusters form early and ligands of semimetals such as S, As, Sb and Te can bond with these clusters constituting embryos for further crystal growth (Junge et al., 2015; Okrugin, 2011; Tredoux et al., 1995). These nanometer-sized PGMs are observed in various geological settings ranging from ophiolites and layered intrusions (Baurier-Aymat et al., 2019; González-Jiménez et al., 2018, 2019, 2020; González-Jiménez and Reich, 2017; Helmy et al., 2013; Junge et al., 2015; Pushkarev et al., 2018; Rivera et al., 2018; Wirth et al., 2013). The primary PGMs can be altered and reworked at lower temperatures. Heavy mineral concentrates are also of great economic importance as the occurrence of the PGMs guides the exploration towards the primary source. For example, the encounter of PGM nuggets on the farm Maandagshoek led to the discovery of the major PGE deposits of the Bushveld Complex (Cawthorn, 1999; Melcher et al., 2005; Merensky, 1924, 1926; Oberthür et al., 2004, 2014; Wagner, 1929). Therefore, the provenance studies on placers are still an important exploration tool for the discovery of major ore bodies today.

Particles of PGMs in German rivers were identified in the Rhine (Dijkstra et al., 2016; Oberthür et al., 2016) and the Danube and their source regions (Dill et al., 2007, 2009, 2010; Lehrberger, 1997). The Os–Ir–Ru alloys in the Danube, which share similarities to the alloys analyzed here, are thought to be derived from the Teplá–Barrandian unit of the Bohemian Massif, part of which extends into the Bavarian Forest along the Czech–German border (Dill et al., 2009, 2010). However, gold particles are more common than PGMs within stream sediments of the Rhine, Danube and Elbe rivers (Albiez, 1951; Elsner, 2009; Goldenberg, 1988; Hofmann, 1965; Kirchheimer, 1969; Oberthür et al., 2016; Ramdohr, 1965). Gold was extracted on a small scale from German river sediments. For example, 363.3 kg of gold was delivered from the Rhine to the Karlsruhe Mint from 1748 to 1874 (Elsner, 2009). The gold contents of the gravels from the Rhine are estimated to be 0.05–11 mg $t^{-1}$ (Elsner, 2009).

The aims of this study are the characterization of PGMs and gold particles collected from stream sediments of the Elbe by scanning electron microscopy with automated mineralogy software using Mineral Liberation Analysis (MLA) and quantitative analysis of the mineral chemistry of individual PGM grains by electron microprobe (EPMA), as well as the evaluation of the potential source area for these precious minerals and the effect of transportation and alteration on the PGM and gold particles.

## 2 Geology of the drainage area

The Elbe and Vltava river system covers a large drainage area. Besides the Vltava, other large tributaries of the Elbe are the Havel (24 000 km$^2$), Saale (24 000 km$^2$), Mulde (7400 km$^2$), Eger/Ohře (5600 km$^2$) and Elster (5500 km$^2$) rivers (Scholz et al., 2005). The Vltava merges with the Elbe at Mělník and is the longest river in the Czech Republic and discharges via the Elbe through Germany into the North Sea (Fig. 1). The Vltava is 430 km long and drains over an area of about 28 000 km$^2$ (Hejzlar et al., 1996; Knab et al., 2006; Rosendorf et al., 2016). The source of the Vltava is located in the Šumava National Park in the Bohemian Massif. The drainage area of Vltava includes various geological formations of the Bohemian Massif, which is a highly deformed metamorphic zone (Moldanubian Zone of the Variscan orogeny) containing geological units of ortho- and paragneisses, migmatites, ultrabasites, and granitoids (Janoušek et al., 1995). Near the confluence with the Elbe, mainly sedimentary rocks of the North Bohemian Basin exist (Walter, 1995). The source of the Elbe is located in the Krkonoše mountains in Czech Republic, intersecting granites, sediments, and volcanic and metamorphic rocks (Hladil et al., 2003; Pašava et al., 2015; Plasil et al., 2009). Further downstream the Elbe covers various additional geological units such as the gabbroic and ultramafic rocks of the Lusatia (Járóka et al., 2019, 2021) and sedimentary, plutonic and metamorphic rocks, including the Erzgebirge and the Granulitgebirge (Hofmann et al., 2018; Zieger et al., 2019).

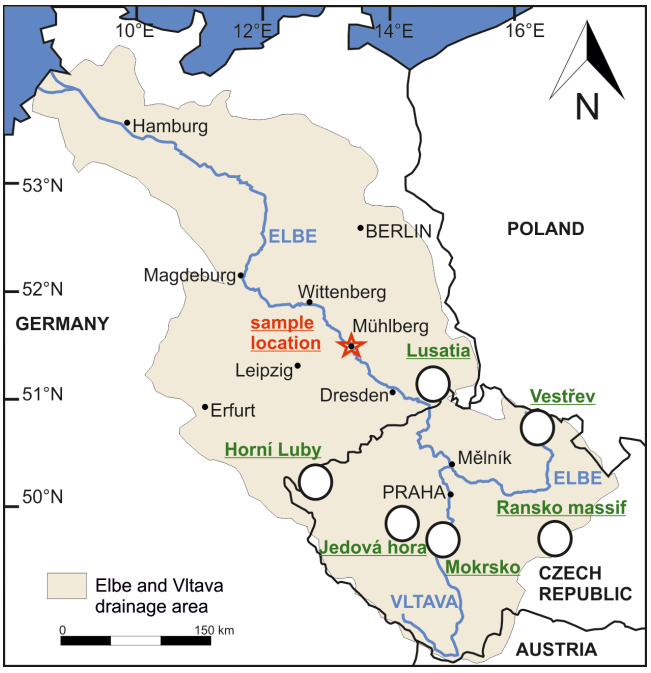


**Figure 1.** Overview map of the Elbe and Vltava drainage system based on Vink et al. (1999) with the sample area and the potential source areas of the Lusatia block (Angstberg, Sohland-Rožany and Kunratice), the Ransko Massif and the Vestřev placer. The Horní Luby and the Jedová Hora are known for cinnabar mineralization, and the Mokrsko is one example for gold mineralization.

## 3 Samples and analytical methods

Two polished sections were produced from heavy mineral concentrates with grain size fractions of $< 63$ and $> 63$ µm, respectively (Fig. 2). The heavy mineral concentrates were separated by shaking tables and heavy mineral separation from a gravel quarry of the Elbe at Mühlberg (51.4528° N, 13.1817° E; Fig. 1) in eastern Germany. The $< 2$ mm fraction of the gravel production was run over carpet sluice. Density separation of the particles attached to the carpet was done using an oscillating table to separate minerals with lower density (e.g., quartz, tourmaline). A hand magnet was used to separate magnetic minerals such as magnetite. In order to obtain a concentrate rich in PGMs, most of the gold was separated by flotation (diesel combined with a frother, i.e., palm oil). Some amounts of gold still remained in the concentrate, but this procedure allowed us to further upgrade the amount of PGMs. Zircons and chromite could be separated from the concentrate by panning. The concentrates were embedded in epoxy resin, followed by stepwise grinding and polishing. Mineral grains are investigated by reflected light microscopy to demonstrate the variety of grains and alteration (Figs. 3, 4). The polished blocks containing mineral grains were qualitatively analyzed using a scanning electron microscope (SEM) coupled with energy-dispersive X-ray spectrometry (EDX).

Quantitative mineralogical analysis was carried out using a FEI Quanta 650F field emission gun scanning electron microscope (FE-SEM) equipped with two Bruker Quantax X-Flash 5030 energy dispersive X-ray spectrometers (EDX) and Mineral Liberation Analysis (MLA) software (suite 3.1.4) for data acquisition at the Federal Institute for Geosciences and Natural Resources (BGR) in Hanover. In the last decade various studies have provided in-depth information on the MLA system and PGM identification (Bachmann et al., 2017; Fandrich et al., 2007; Gu, 2003; Osbahr et al., 2015). In this study, the GXMAP (grain-based X-ray mapping) measurement mode was applied for identification of PGM grains with high spatial resolution and accuracy (Fandrich et al., 2007).

Following SEM analysis, grains of interest were subsequently measured by electron probe microanalysis (EPMA) using a JEOL JXA-8530F microprobe at the Federal Institute for Geosciences and Natural Resources (BGR) in Hanover. The analytical conditions were set to focused electron beam with an acceleration voltage and beam current of 30 kV and 40 nA, respectively. For PGM and gold analysis, the respective X-ray line, measuring time on peak in seconds, spectrometer crystal, reference material and mean detection limit

for each element were as follows (ordered by atomic number): S K$\alpha$ (PET, 10 s, HgS for cinnabar, artificial $Pt_{0.7}Pd_{0.3}S$ for PGE sulfides, and $FeS_2$ for all other unknowns, 202 ppm), Fe K$\alpha$ (LIFL, 10 s, metal, 83 ppm), Ni K$\alpha$ (LIFL, 40 s, metal, 40 ppm), Cu K$\alpha$ (LIFH, 60 s, metal, 39 ppm), As L$\alpha$ (TAP, 20 s, synthetic GaAs, 233 ppm), Ru L$\alpha$ (PETH, 40 s, metal, 317 ppm), Rh L$\alpha$ (PETH, 20 s, metal, 386 ppm), Pd L$\alpha$ (PETH, 20 s, metal, 451 ppm), Ag L$\alpha$ (PETH, 40 s, metal, 322 ppm), Sn L$\alpha$ (PET, 40 s, metal, 234 ppm), Sb L$\alpha$ (PET, 40 s, metal, 225 ppm), Te L$\alpha$ (PET, 40 s, metal, 216 ppm), Os L$\alpha$ (LIFH, 40 s, metal, 134 ppm), Ir L$\alpha$ (LIFH, 40 s, metal, 143 ppm), Pt L$\alpha$ (LIFH, 20 s, metal, 220 ppm), Au L$\alpha$ (LIFL, 20 s, metal, 197 ppm), Hg L$\alpha$ (LIFL, 80 s, HgS, 111 ppm) and Bi M$\alpha$ (PETH, 40 s, metal, 423 ppm). The mean atomic number (MAN) correction of the ProbeSoftware package was applied for correction of background, and raw data were corrected using the phi–rho–z method supplied by ProbeSoftware package.

## 4 Results

### 4.1 Morphologies and composition of gold and PGM grains

Particle sizes of gold and PGM are up to 600 µm in diameter and range from irregular to rounded shapes (Figs. 3, 4). Gold particles often have an Ag-poor rim and an Ag-rich core as shown by zoning of individual particles (Fig. 3c, e). Additionally, Hg-rich (Figs. 3a, d, e, 4b), Cu-rich gold grains occur (Figs. 3d, 4d), and few gold grains contain Pd (Fig. 4f). Similarly, PGM particles commonly have different compositions of their core and rim as evidence for multiphase grains and alteration (Fig. 3a, b). Inclusions of PGM within individual PGM particles are also frequently observed (Fig. 3a, d, e). Figure 3a and b show sperrylite cores with rims of pure platinum. Different alloys of Os–Ir–Ru are shown in Figs. 3e and 4b, c, d and f. Additionally, Ir–Os–Ru alloys occur as different particles with variable grain sizes (Fig. 4b, c, d, e, f). Similarly, Ru–Os–Ir alloys dominated by Ru are shown in Figs. 3b, 4b and f. Apart from IPGE (Os, Ir, Ru) alloys, also Pt–Fe alloys are frequently found (Figs. 3e, 4). Figure 4b shows a particle of native platinum. Other PGM are PGE sulfides (Fig. 4e), sperrylite (Fig. 4) and rustenburgite (Fig. 4e).

### 4.2 Compositions and abundance of gold and PGM grains

Analysis carried out by MLA showed that, in addition to gold and PGM particles, heavy minerals such as cassiterite, ferberite, monazite, uraninite, columbite–tantalite, magnetite, cinnabar and zircon are present in the heavy mineral concentrates (Fig. 5). Both grain size fractions $< 63$ and $> 63$ µm show similar percentage by area of heavy mineral abundance.

For $< 63$ µm fraction, the most abundant minerals (expressed in area %) are cassiterite (71 %) and wolframite (12 %). The general group of other oxides (e.g., uraninite, magnetite, columbite–tantalite), monazite and zircon is 6.2 area %. The percentage of the gold and PGM particles is 0.6 area % and 6.7 area %, respectively. Platinum-group minerals are sperrylite (2 area %), PGE Fe (1.6 area %), PGE alloys (2.9 area %) and PGE sulfides (0.1 area %). By looking only at the PGM proportion, it is obvious that Os–Ir–Ru alloys are the most frequent PGM (42.9 %), followed by sperrylite (31.1 %), Pt–Fe alloys (23.4 %) and PGE sulfides (2.6 %).

Similarly, to the smaller fraction, the most abundant minerals in the grain size fraction $> 63$ µm are cassiterite (58 area %) and wolframite (24 area %). The general group of oxides (e.g., uraninite, magnetite, columbite–tantalite), monazite and zircon is 6.7 area %. Due to the processing technique as described above also in the $> 63$ µm, the PGMs are more abundant than gold; i.e., gold particles are 2.7 area % and PGM 4.5 area %. Platinum-group minerals are sperrylite (2.4 area %), PGE Fe (1.0 area %), PGE alloys (1.1 area %) and PGE sulfides ($< 0.1$ area %). Regarding PGM proportion, sperrylite is the most frequent PGM (54.9 %), followed by Os–Ir–Ru alloys (23.2 %), Pt–Fe alloys (21.0 %) and PGE sulfides (0.9 %).

### 4.3 Mineral chemistry of Os–Ir–Ru–Pt alloys

Representative analyses of Os–Ir–Ru–Pt alloys are shown in Table 1. Os–Ir–Ru–Pt alloys form a mineral group with far-reaching substitution shown in ternary variation diagrams (Fig. 6a, b). Mineral names based on their chemistry and crystallography are ruthenium, osmium, iridium and rutheniridosmium (Harris and Cabri, 1991). Ruthenium, osmium and rutheniridosmium are hexagonal, whereas iridium is cubic (Cabri, 2002). For comparison Os–Ir–Ru–(Pt) alloys from ophiolites (Hagen et al., 1990; Shcheka et al., 2004; Tolstykh et al., 2002b), Uralian–Alaskan-type complexes (Malitch et al., 2002; Tolstykh et al., 2002a, b) and the Rhine (Oberthür et al., 2016) are plotted in Fig. 6.

In total 146 Os–Ir–Ru–(Pt) alloys were analyzed by EPMA (Fig. 6a, b). The Ru concentrations range from 0.12 atom % to 69.47 atom %. The median values of Os and Ir are higher than for Ru (36.65 atom % and 34.90 atom %, respectively). A negative correlation exists between Os and Ir particularly for alloys with Ru concentrations $< 33$ atom % (Fig. 7a). Similarly, Ru shows a negative correlation with Ir (Fig. 7b). The Fe concentrations are generally below the detection limit but occasionally range up to 9.39 atom %. The alloys containing higher Fe concentrations correlate positively with Ir (Fig. 7c). However, negative correlations exist between Fe and Os (Fig. 7d). Rhodium concentrations are generally below the detection limit but range up to 8.76 atom %. Particles that contain measurable concentrations of Pt are typically Ir-rich, Ru-poor and Os-poor (Fig. 6b). The Pt concentrations range from below the detection limit up to 26.82 atom %.

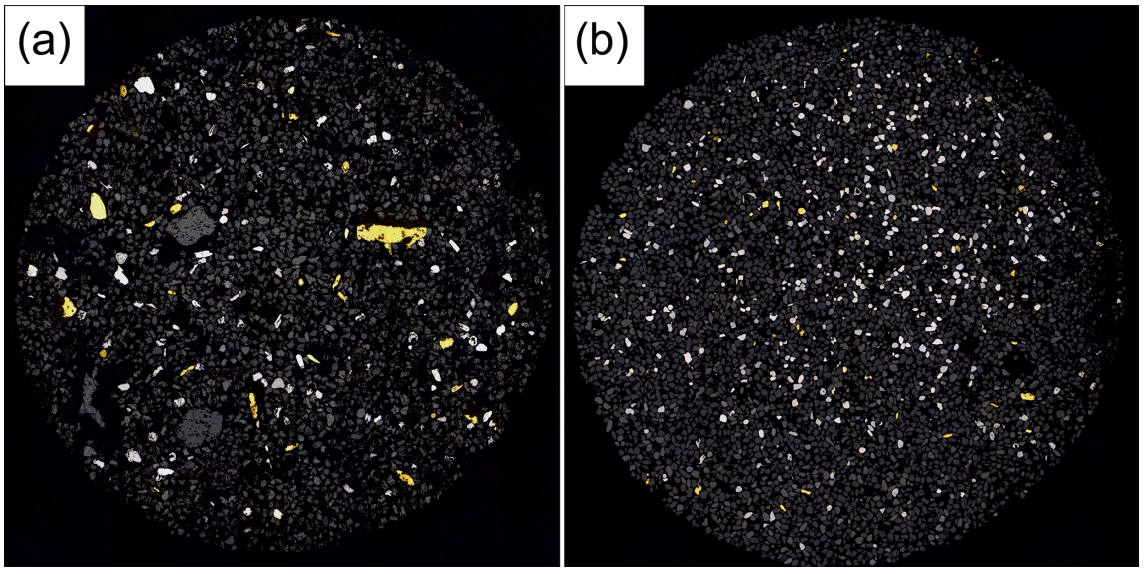


**Figure 2.** Overview images of the polished sections from the heavy mineral concentrates. **(a)** The fraction > 63 µm with larger gold grains (yellow) and platinum-group minerals (white). **(b)** Fraction < 63 µm. Image widths each 5 mm.

### 4.4 Pt–Fe alloys and Pd–Fe alloys

In total 122 Pt–Fe alloys are analyzed showing a broad range of compositional variation (Table 1). The Pt–Fe alloys are grouped into (1) native platinum (> 80 atom %), (2) ferroan Pt (20 atom % to 50 atom % Fe), (3) isoferroplatinum (2.64 to 3.04 apfu of PGE), (4) tetraferroplatinum group with Ni + Cu + Fe ≈ 50 atom % and (5) PGE-(Fe,Cu,Ni) alloys plotting in the phase field of $\gamma$ (Pt,Fe) with sum PGE > 3.04 apfu. This classification is based on the work of Cabri and Feather (1975), which was recently reviewed and updated by Cabri et al. (2022b). Isoferroplatinum can only be correctly classified by X-ray diffraction, but it is still considered here based on the concentrations of PGE and Fe according to the classification by Cabri et al. (2022b).

The Pt–Fe alloys are Pt-rich ranging from 23.47 atom % to 77.98 atom % (median: 64.27 atom %). The Fe contents range from 4.31 atom % to 33.11 atom % (median: 26.89 atom %). Palladium concentrations are generally close to the detection limit. However, maximum Pd values range up to 46.38 atom %. Figure 8a shows a negative correlation between Pt and Pd. Similarly, Rh is mostly at the level of the detection limit except some particles showing Rh concentrations of up to 15.63 atom %. Iridium concentrations are mainly at or close to the detection limit, but occasionally maximum Ir concentrations of 9.67 atom % are analyzed. Ruthenium values above 1 atom % are shown for five particles (maximum 6.11 atom %). Similarly, Os values reach concentrations above the detection limit in six particles (maximum 6.17 atom %). Nickel and Cu are usually close to the detection limit, but maximum values exist of 6.79 atom % and 18.47 atom %, respectively. Figure 8b shows the Pt versus Fe diagram. In Fig. 8c the correlation between the apfu Fe + Cu + Ni and PGE (based on $Z = 4$) shows the compositional continuum between the different groups of the Pt–Fe alloys isoferroplatinum, tetraferroplatinum and ferroan platinum. The boundaries between the groups are indicated by gaps in the continuum as proposed by Cabri et al. (2022b). The ternary diagram in Fig. 8d visualizes the variation of the different PGE-Fe alloys with respect to Cu + Ni and indicates the difference of the single tetraferroplatinum grain compared to the other PGE-Fe alloys of the Elbe.

### 4.5 Native platinum [Pt]

Representative analyses of native platinum particles are shown in Table 1. In total 22 particles with Pt concentrations > 80 atom % are analyzed. The Pt concentrations range from 81.18 atom % to 99.63 atom % (median: 98.63 atom %). Copper, Ni and Fe are usually in range of the respective detection limit. Palladium concentration in one particle is 4.92 atom %; otherwise Pd values are below the detection limit.

### 4.6 Palladium alloys

Also one Pd-rich particle had 11.76 atom % Pd and Pt concentrations of 74.92 atom % (Table 1). Particularly, one particle has concentrations of 73.69 atom % Pd and 17.74 atom % Pt (Table 1).

### 4.7 Sperrylite [$PtAs_2$]

Electron microprobe analysis (n=154) showed that sperrylite is stoichiometric and rather homogenous. Representative analysis of sperrylite is shown in Table 1. Platinum ranges

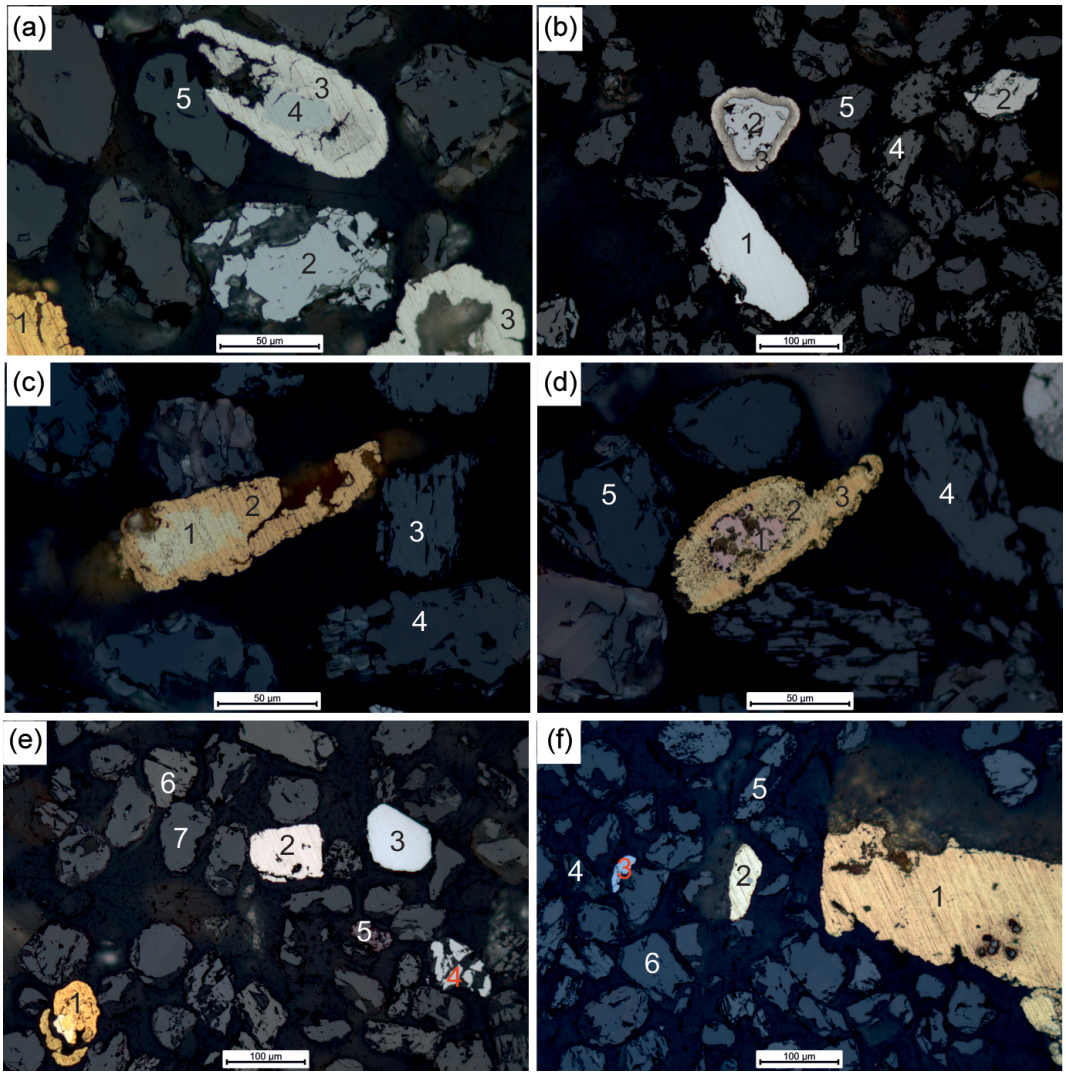


**Figure 3.** Reflected-light photomicrographs of gold grains and PGM in oil of the concentrate > 63 µm. **(a)** (1) pure gold with Hg-bearing gold along rim, (2) sperrylite, (3) native Pt, (4) symplectitic intergrowth of sperrylite and native Pt and (5) cassiterite. **(b)** (1) Ru–Os–Ir alloy, (2) sperrylite, (3) native Pt, (4) wolframite and (5) cassiterite, **(c)** (1) Ag-rich gold, (2) pure gold, (3) wolframite and (4) cassiterite. **(d)** (1) Cu-rich gold (Cu : Au ∼ 1 : 1), (2) Hg–Ag-rich gold, (3) Hg-bearing gold, (4) wolframite and (5) cassiterite. **(e)** (1) Ag- and Hg-rich gold (bright center) with Hg-bearing gold along rim, (2) Pt–Fe alloy, (3) Os–Ir alloy, (4) sperrylite, (5) cinnabar, (6) wolframite and (7) cassiterite. **(f)** (1) Ag-bearing gold, (2) Ag-rich gold with pyrite inclusion, (3) sperrylite, (4) monazite, (5) wolframite and (6) cassiterite.

from 28.11 atom % to 33.49 atom % (median: 32.89 atom %), and the concentrations of As range from 63.65 atom % to 66.59 atom % (median: 66.07 atom %).

### 4.8 Rustenburgite [$Pt_3Sn$]

In total 11 particles showed relatively homogenous composition with Sn concentrations ranging from 22.74 atom % to 25.98 atom % (median: 25.55 atom %) and Pt concentrations ranging from 73.65 atom % to 74.23 atom % (median: 73.92 atom %). A representative analysis of rustenburgite particles is shown in Table 1.

### 4.9 Gold and Au-bearing alloys [Au + Ag,Cu,Hg]

In total 98 Au particles are analyzed, ranging from 39.98 atom % to 99.38 atom % Au (median: 87.26 atom %). These particles range from almost pure Au to Ag- or Cu-bearing Au particles (Table 2). Additionally, Hg above 1 atom % was encountered in 22 particles with maximum values of 26.75 atom %. Four particles hosted Pd concentrations of up to 20.64 atom %, but generally Pd is below the detection limit for majority of gold particles. Copper values above the detection limit range up to 51.01 atom %, and in seven particles Cu is > 1 atom %. Representative analyses of

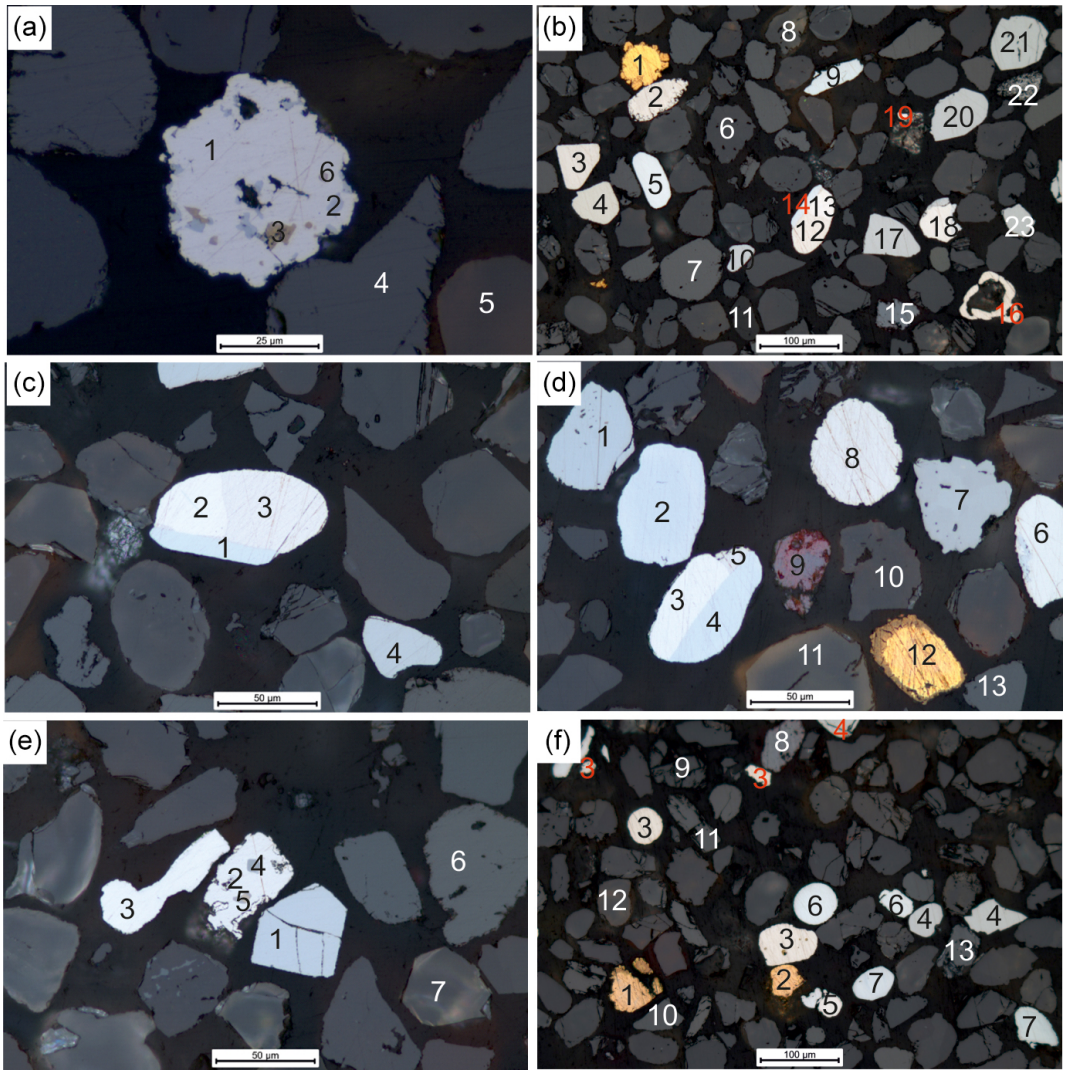


**Figure 4.** Reflected-light photomicrographs of gold grains and PGM in oil of the concentrate < 63 µm. **(a)** (1) Pt–Fe alloy, (2) sperrylite, (3) pyrrhotite–chalcopyrite intergrowth, (4) wolframite, (5) cassiterite and (6) pentlandite. **(b)** (1) Ag-bearing gold with Hg-bearing gold along rim, (2) Pt–Fe alloy, (3) Pt–Fe alloy, (4) rustenburgite, (5) Ru–Os–Ir alloy, (6) cassiterite, (7) wolframite, (8) thorianite, (9) Ru–Os–Ir alloy, (10) sperrylite, (11) monazite, (12) Pt–Fe alloy, (13) Ir–Os–Ru alloy, (14) Os–Ir–Ru alloy, (15) cinnabar, (16) native Pt, (17) sperrylite, (18) Ir–Os–Ru alloy, (19) Ir–Os–Ru alloy, (20) sperrylite, (21) sperrylite, (22) tungsten carbide and (23) sperrylite. **(c)** Higher magnification of image B, (1) Os–Ir–Ru alloy, (2) Pt–Fe alloy, (3) Ir–Os–Ru alloy and (4) sperrylite. **(d)** (1) Sperrylite, (2) Os–Ir–Ru alloy, (3) Ir–Os–Ru alloy, (4) Os–Ir–Ru alloy, (5) Pt–Fe alloy, (6) Ir–Os–Ru alloy, (7) tungsten carbide, (8) Pt–Fe alloy, (9) cinnabar, (10) cassiterite, (11) thorianite and (12) Cu-rich gold with Hg-bearing gold along rim. **(e)** (1) Sperrylite, (2) Pt–Fe alloy, (3) Ir–Os alloy, (4) PGE sulfide, (5) pentlandite, (6) wolframite and (7) cassiterite. **(f)** (1) Pd-rich gold with Hg-bearing gold along rim, (2) pure gold, (3) Pt–Fe alloy, (4) sperrylite, (5) Ir–Os–Ru alloy, (6) Ru–Os–Ir alloy, (7) Os–Ir–Ru alloy, (8) cinnabar, (9) thorianite, (10) columbite–tantalite, (11) wolframite, (12) cassiterite and (13) stolzite.

gold particles (Ag-rich, Ag-poor, Hg-rich and Cu–Pd-rich) are shown in Table 1.

### 4.10 Cinnabar [HgS]

In addition to PGM and Au particles, 54 cinnabar particles are analyzed. The majority of the cinnabar particles are rather porous. Measurements of apparently non-porous spots of the particles show a relatively homogenous distribution of Hg ranging from 49.07 atom % to 53.21 atom % (median: 51.13 atom %) and S ranging from 46.64 atom % to 50.80 atom % (median: 48.54 atom %).

## 5 Discussion

The Elbe and Vltava have large drainage areas with different geological lithologies. So far, studies have focused mainly on

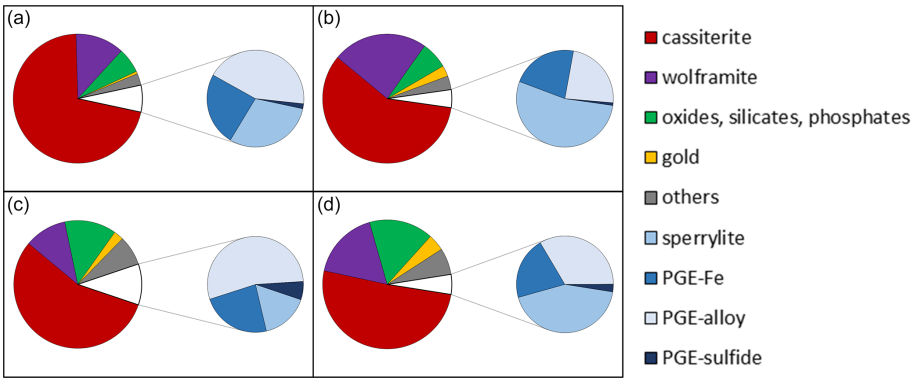


**Figure 5.** Results of the measurements of the Mineral Liberation Analysis of the respective concentrate. **(a)** < 63 µm fraction [in area %]. **(b)** > 63 µm fraction [in area %]. **(c)** < 63 µm fraction [in particle abundance]. **(d)** > 63 µm fraction [in particle abundance].

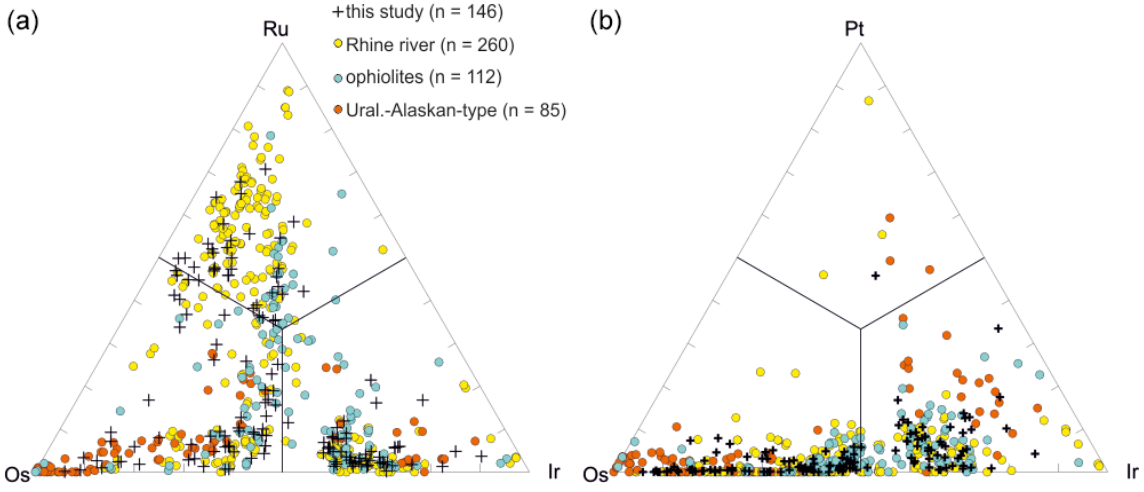


**Figure 6.** Compositional variation of Ru–Os–Ir–Pt alloys ($n = 146$). **(a)** Ru–Os–Ir alloys. **(b)** Ir–Pt–Os alloys. Orange denotes Uralian–Alaskan-type complexes ($n = 85$; Malitch et al., 2002; Tolstykh et al., 2002a, b). Blue denotes ophiolites ($n = 112$; Hagen et al., 1990, Tolstykh et al., 2002b, Shcheka et al., 2004). Yellow denotes the Rhine ($n = 260$; Oberthür et al., 2016).

transparent minerals within the Elbe and Vltava, and investigations of opaque minerals such as gold and PGM are very rare (Gutzmer et al., 2013; Kaufmann and Lehmann, 2016; Lehmann, 2010). Heavy mineral concentrates in this study from the Elbe revealed gold and PGM particles of different shapes and chemical composition, as well as various degrees of alteration processes. The differences in chemical compositions and morphological features argue for multiple events from low to high temperatures and different source regions. Placer deposits of PGM exist worldwide, and the chemical compositions and morphology of individual grains are described in detail combined with provenance studies (Cabri et al., 1996, 2022a; Weiser, 2002). Compositional variation of PGM can also provide further evidence for formation processes as well as mineral chemical properties including miscibility gaps and element substitutions. Therefore, distinct features of individual PGM groups can provide evidence for the geological setting of the source region as well as post-magmatic processes affecting both physical and chemical properties of the particles.

### 5.1 Chemical zoning of gold particles

Typically, the zoning of gold particles consisting of Ag-rich cores and Ag-poor rims (Fig. 3c, e) can be explained by the greater mobility of Ag relative to Au under pH and Eh conditions present in meteoric environment as well as in laterites (Bowles, 1986; Fairbrother et al., 2012; Mann, 1984; Reith et al., 2012). This observation was described in various placer and laterite studies worldwide (Bowell, 1992; Desborough, 1970; Groen et al., 1990; Larizzatti et al., 2008; Oberthür et al., 2016; Suh and Lehmann, 2003) and confirmed here for the Elbe as well.

Copper-rich gold particles are well known in the literature (Chapman et al., 2009, 2021; Moles et al., 2013), and the order–disorder are described in the Au–Cu phase diagram

**Table 1.** Representative EPMA analysis of selected PGM particles (in wt %, atom % and apfu); bdl – below detection limit.

| | | Fe | Ni | Cu | As | Ru | Rh | Pd | Sn | Os | Ir | Pt | Sum |
|---|---|---|---|---|---|---|---|---|---|---|---|---|---|
| wt % | | | | | | | | | | | | | |
| Elbe < 63 µm MLA_183 | ferroan Pt | 12.86 | 0.16 | 1.56 | bdl | 0.16 | 0.33 | 3.37 | bdl | 0.11 | 2.96 | 78.86 | 100.38 |
| Elbe < 63 µm MLA_352a | isoferroplatinum | 9.84 | 0.363 | 1.21 | bdl | bdl | bdl | 0.94 | 0.05 | 0.99 | 1.39 | 84.93 | 99.72 |
| Elbe < 63 µm MLA_102 | tetraferroplatinum | 14.48 | 3.30 | 4.26 | bdl | 0.11 | 1.67 | 8.75 | bdl | 0.14 | 4.94 | 62.40 | 100.05 |
| Elbe < 63 µm MLA_107 | $\gamma$(Pt,Fe) | 6.32 | bdl | 0.97 | bdl | 0.18 | 1.17 | 2.17 | bdl | 0.19 | 2.34 | 86.64 | 100.09 |
| Elbe < 63 µm MLA_301a | Pd alloy | 1.45 | bdl | 1.64 | bdl | 0.17 | 0.91 | 66.15 | 0.25 | bdl | 0.86 | 29.18 | 101.17 |
| Elbe < 63 µm MLA_063 | Pt alloy | 1.35 | 0.02 | 1.59 | bdl | 0.24 | 1.03 | 7.34 | 0.09 | 0.36 | 2.60 | 85.77 | 100.40 |
| Elbe < 63 µm MLA_219 | Os–Ir–Ru–Pt | 0.02 | bdl | 0.02 | bdl | 3.94 | 0.09 | 0.14 | 0.06 | 84.29 | 12.32 | 0.34 | 101.21 |
| Elbe > 63 µm MLA_143a | Os–Ir–Ru–Pt | 0.03 | bdl | bdl | bdl | 32.51 | 0.47 | 0.32 | 0.04 | 51.31 | 16.19 | 0.21 | 101.23 |
| Elbe < 63 µm MLA_274 | Os–Ir–Ru–Pt | 0.15 | 0.04 | 0.03 | bdl | 0.84 | 0.50 | 0.12 | bdl | 31.05 | 65.54 | 3.41 | 101.75 |
| Elbe > 63 µm MLA_115a | Os–Ir–Ru–Pt | 3.11 | bdl | 0.30 | bdl | 1.22 | 4.09 | 0.28 | 0.07 | 4.94 | 55.99 | 31.02 | 101.14 |
| Elbe < 63 µm MLA_366 | sperrylite | bdl | 0.07 | bdl | 42.99 | 0.30 | bdl | 0.34 | bdl | bdl | 0.08 | 56.03 | 100.19 |
| Elbe < 63 µm MLA_030 | rustenburgite | 0.09 | bdl | bdl | bdl | bdl | bdl | bdl | 17.65 | bdl | bdl | 82.78 | 100.52 |
| atom % | | | | | | | | | | | | | |
| Elbe < 63 µm MLA_183 | ferroan Pt | 32.23 | 0.38 | 3.44 | bdl | 0.22 | 0.45 | 4.44 | bdl | 0.08 | 2.16 | 56.60 | 100 |
| Elbe < 63 µm MLA_352a | isoferroplatinum | 26.75 | 0.93 | 2.88 | bdl | bdl | bdl | 1.35 | 0.07 | 0.79 | 1.10 | 66.12 | 100 |
| Elbe < 63 µm MLA_102 | tetraferroplatinum | 31.31 | 6.79 | 8.08 | bdl | 0.13 | 1.96 | 9.93 | bdl | 0.09 | 3.10 | 38.61 | 100 |
| Elbe < 63 µm MLA_107 | $\gamma$(Pt,Fe) | 18.26 | bdl | 2.46 | bdl | 0.29 | 1.83 | 3.28 | bdl | 0.16 | 1.97 | 71.66 | 100 |
| Elbe < 63 µm MLA_301a | Pd alloy | 3.08 | bdl | 3.06 | bdl | 0.20 | 1.05 | 73.69 | 0.25 | bdl | 0.53 | 17.74 | 100 |
| Elbe < 63 µm MLA_063 | Pt alloy | 4.12 | 0.07 | 4.26 | bdl | 0.41 | 1.70 | 11.76 | 0.13 | 0.33 | 2.31 | 74.92 | 100 |
| Elbe > 63 µm MLA_011 | native Pt | bdl | 0.03 | bdl | bdl | 0.24 | 0.15 | bdl | 0.10 | bdl | bdl | 99.31 | 100 |
| Elbe < 63 µm MLA_219 | Os–Ir–Ru–Pt | 0.07 | bdl | 0.06 | bdl | 7.07 | 0.16 | 0.23 | 0.09 | 80.38 | 11.62 | 0.31 | 100 |
| Elbe > 63 µm MLA_143a | Os–Ir–Ru–Pt | 0.08 | bdl | bdl | bdl | 46.85 | 0.66 | 0.43 | 0.05 | 39.29 | 12.27 | 0.16 | 100 |
| Elbe < 63 µm MLA_274 | Os–Ir–Ru–Pt | 0.51 | 0.13 | 0.09 | bdl | 1.53 | 0.89 | 0.22 | bdl | 30.19 | 63.07 | 3.24 | 100 |
| Elbe > 63 µm MLA_115a | Os–Ir–Ru–Pt | 9.39 | bdl | 0.81 | bdl | 2.03 | 6.71 | 0.44 | 0.10 | 4.38 | 49.13 | 26.82 | 100 |
| Elbe < 63 µm MLA_366 | sperrylite | bdl | 0.14 | bdl | 65.81 | 0.34 | bdl | 0.37 | bdl | bdl | 0.05 | 32.94 | 100 |
| Elbe < 63 µm MLA_030 | rustenburgite | 0.27 | bdl | bdl | bdl | bdl | bdl | bdl | 25.88 | bdl | bdl | 73.85 | 100 |
| apfu | | | | | | | | | | | | | |
| Elbe < 63 µm MLA_183 | ferroan Pt | 1.29 | 0.02 | 0.14 | | 0.01 | 0.02 | 0.18 | | 0.00 | 0.09 | 2.26 | 4 |
| Elbe < 63 µm MLA_352a | isoferroplatinum | 1.07 | 0.04 | 0.12 | | | | 0.05 | 0.00 | 0.03 | 0.04 | 2.64 | 4 |
| Elbe < 63 µm MLA_102 | tetraferroplatinum | 1.25 | 0.27 | 0.32 | | 0.01 | 0.08 | 0.40 | | 0.00 | 0.12 | 1.54 | 4 |
| Elbe < 63 µm MLA_107 | $\gamma$(Pt,Fe) | 0.73 | | 0.10 | | 0.01 | 0.07 | 0.13 | | 0.01 | 0.08 | 2.87 | 4 |
| Elbe < 63 µm MLA_301a | Pd alloy | 0.12 | | 0.12 | | 0.01 | 0.04 | 2.95 | 0.01 | | 0.02 | 0.71 | 4 |
| Elbe < 63 µm MLA_063 | Pt alloy | 0.16 | 0.00 | 0.17 | | 0.02 | 0.07 | 0.47 | 0.01 | 0.01 | 0.09 | 3.00 | 4 |
| Elbe > 63 µm MLA_011 | native Pt | | 0.00 | | | 0.00 | 0.00 | | 0.00 | | | 0.99 | 1 |
| Elbe < 63 µm MLA_219 | Os–Ir–Ru–Pt | 0.00 | | 0.00 | | 0.07 | 0.00 | 0.00 | 0.00 | 0.80 | 0.12 | 0.00 | 1 |
| Elbe > 63 µm MLA_143a | Os–Ir–Ru–Pt | 0.00 | | | | 0.47 | 0.01 | 0.00 | 0.00 | 0.39 | 0.12 | 0.00 | 1 |
| Elbe < 63 µm MLA_274 | Os–Ir–Ru–Pt | 0.01 | 0.00 | 0.00 | | 0.02 | 0.01 | 0.00 | | 0.30 | 0.63 | 0.03 | 1 |
| Elbe > 63 µm MLA_115a | Os–Ir–Ru–Pt | 0.09 | | 0.01 | | 0.02 | 0.07 | 0.00 | 0.00 | 0.04 | 0.49 | 0.27 | 1 |
| Elbe < 63 µm MLA_366 | sperrylite | | 0.00 | | 1.97 | 0.01 | | 0.01 | | | 0.00 | 0.99 | 3 |
| Elbe < 63 µm MLA_030 | rustenburgite | 0.01 | | | | | | | 1.04 | | | 2.95 | 4 |

(Okamoto et al., 1987). A few studies analyzed Pd-bearing gold particles (Chapman et al., 2009, 2017).

Some gold particles contain Hg-rich rims (Figs. a, e, 4d, f). It is generally assumed that most Hg found in Au placers is a result of pollution from the amalgamation process used during Au extraction or other anthropogenic influences (Kinnunen, 2003; Pfeiffer et al., 1989, 1993). However, Hg-rich gold particles were also observed in natural samples (Chapman et al., 2009, 2010, 2017, 2021; Kinnunen, 2003; Knight et al., 1999; Oberthür and Saager, 1986). One possible explanation for these Hg-rich gold particles is an anthropogenic influence (Chapman et al., 2021). However, for Hg-rich gold particles from the Witwatersrand in South Africa, the source of Hg is assumed to be the surrounding sediments followed by local mobilization of Hg and amalgamation of the gold (Oberthür and Saager, 1986). Natural Au–Ag–Hg alloys were found in the Las Cruces ore deposit, in the eastern part of the Iberian Pyrite Belt located in a strongly leached black shale horizon (Yesares et al., 2014). In Las Cruces, supergene processes are assumed to be the main source for Hg-rich gold particles (Yesares et al., 2014). Experimental studies showed that the mobilization of Hg during the dissolution of cinnabar is sufficient to form natural Au–Hg amalgam in downstream placer settings (Holley et al., 2007). Therefore the natural dissolution of cinnabar can be expected in oxidative, fluvial environments (Holley et al., 2007). Similarly, experiments on a simulated stream sediment showed that Hg

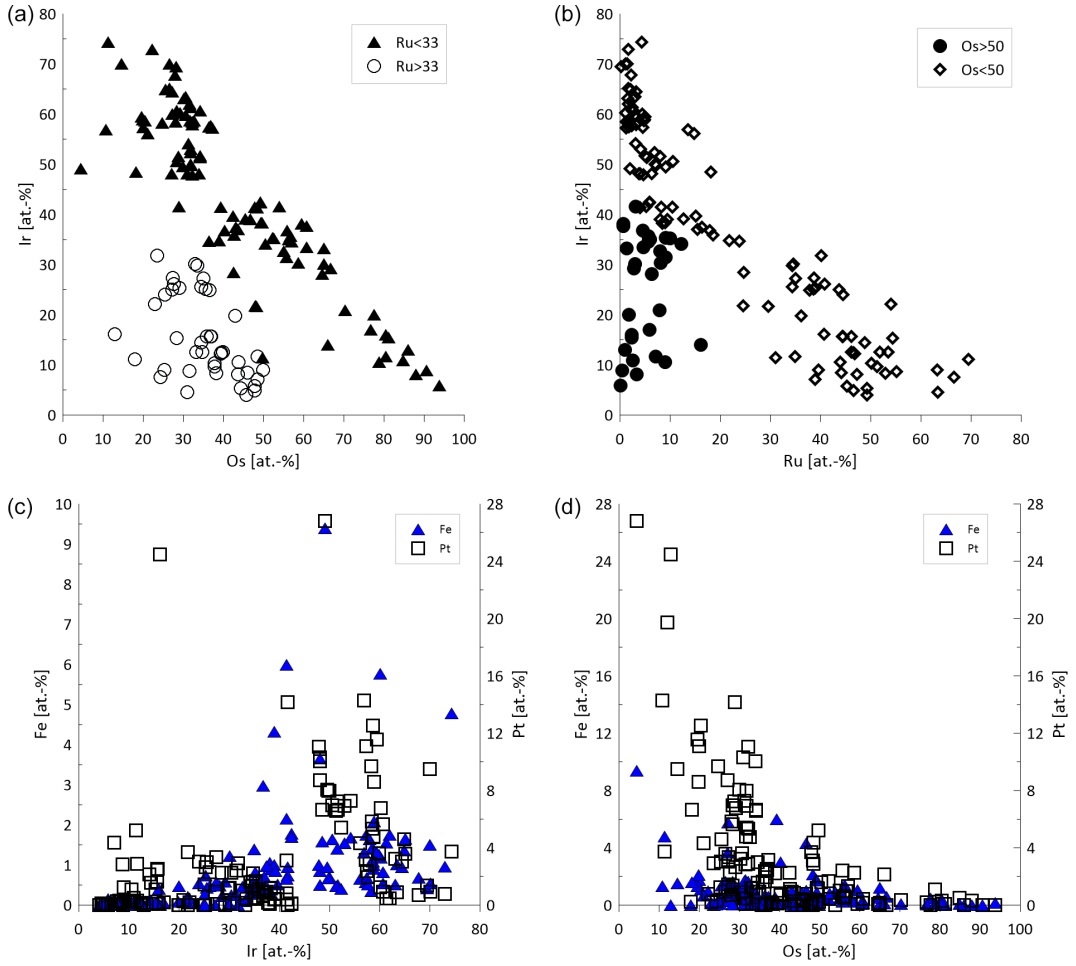


**Figure 7.** Compositional variation of Os–Ir–Ru–(Pt) alloys ($n = 146$). **(a)** Ir and Os concentrations showing two groups of Ru > 33 atom % and Ru < 33 atom %. **(b)** Correlation between Ir and Ru for alloys with Os concentrations < 50 atom % and no correlation for alloys with Os values > 50 atom %. **(c)** Fe and Ir concentrations showing correlation of Fe and Pt with Ir. **(d)** Fe and Os concentrations, where Fe and Pt are generally associated with alloys of low Os concentrations.

can be released in a stream environment and form Hg–Au alloys along rims of gold particles (Miller et al., 2002).

For the Hg-rich gold particles of the Elbe it can be assumed that Hg was mobilized from the cinnabar causing in situ amalgamation of the gold particles, which results in Hg-rich rims. Therefore, the in situ amalgamation of the gold particles is assumed to be the result of natural processes of associated gold and cinnabar particles in the placer. Additionally, the amalgamation of the gold particles can take place during the transportation of the particles, either as a reaction with cinnabar or with anthropogenic Hg in the river system.

### 5.2 Abundances and distribution of PGM in the Elbe

It was shown previously by Oberthür et al. (2016) that within the Rhine the PGM assemblage is dominated by Ru–Os–Ir alloys (69.6 %), Pt–Fe alloys (14.9 %), sperrylite (9.4 %) and other PGMs (together 7.2 %). In the Rhine, these authors did not observe any Rh- and Pd-dominated PGM or any PGE sulfides (except for rare grains of laurite–erlichmanite). In the Danube, frequent occurrence of Ir–Os alloys is described as well (Dill et al., 2009). Similarly to the present study from the Elbe, Os–Ir–Ru alloys, as well as Pt–Fe alloys and sperrylite, are the most frequent PGMs; other PGMs such as PGE sulfides and sulfarsenides are rare (Table 3). In this work we used area % instead of frequency data, as area % provides more accurate information on the entire platinum-group mineral budget rather than simple particle counting. Therefore, due to the larger average particle size, sperrylite is underestimated by looking at frequency data (Fig. 5). On the other hand, PGE alloys are overestimated compared to area % (Fig. 5). Nevertheless, the relative abundance of the platinum-group minerals is still comparable.

The heavy mineral concentrates of the Elbe showed that Ru–Os–Ir alloys, Pt–Fe alloys and sperrylite are the most

**Table 2.** Composition of representative gold particles (in wt %, atom % and calculated apfu based on $Z = 1$). Compositional differences exist between Ag-rich cores, Ag-poor rims, Hg-rich rims and one Cu–Pd gold particle.

| | | Cu | Pd | Ag | Au | Hg | Sum |
|---|---|---|---|---|---|---|---|
| wt % | | | | | | | |
| Elbe > 63 µm MLA_188a | gold | bdl | bdl | 0.72 | 99.73 | 0.05 | 100.82 |
| Elbe > 63 µm MLA_177 | gold (Ag) | 0.02 | 0.14 | 8.79 | 90.10 | 1.00 | 100.78 |
| Elbe > 63 µm MLA_166a | Cu–Au alloy | 26.05 | 1.55 | 0.47 | 72.89 | 0.26 | 101.58 |
| Elbe > 63 µm MLA_192 | gold (Hg) | bdl | bdl | bdl | 76.76 | 22.20 | 99.88 |
| atom % | | | | | | | |
| Elbe > 63 µm MLA_188a | gold | bdl | bdl | 1.29 | 98.09 | 0.05 | 100 |
| Elbe > 63 µm MLA_177 | gold (Ag) | 0.06 | 0.24 | 14.75 | 83.00 | 0.90 | 100 |
| Elbe > 63 µm MLA_166a | Cu–Au alloy | 51.01 | 1.82 | 0.55 | 46.14 | 0.16 | 100 |
| Elbe > 63 µm MLA_192 | gold (Hg) | 0.00 | 0.00 | 0.00 | 76.22 | 21.61 | 100 |
| apfu | | | | | | | |
| Elbe > 63 µm MLA_188a | gold | | | 0.01 | 0.98 | 0.00 | 1 |
| Elbe > 63 µm MLA_177 | gold (Ag) | 0.00 | 0.00 | 0.15 | 0.83 | 0.01 | 1 |
| Elbe > 63 µm MLA_166a | Cu–Au alloy | 0.51 | 0.02 | 0.01 | 0.46 | 0.00 | 1 |
| Elbe > 63 µm MLA_192 | gold (Hg) | bdl | bdl | bdl | 0.76 | 0.22 | 1 |

frequent PGMs. However, PGE bismuthotellurides and PGE sulfides (such as cooperite/braggite and laurite) are very rare. Similar PGM assemblages as found in the Elbe have been described from ophiolite-hosted chromitites and associated placer deposits worldwide (Economou-Eliopoulos, 1996; González-Jiménez et al., 2009; Tolstykh et al., 2009; Weiser, 2002) as well as Uralian–Alaskan-type intrusions (Barkov et al., 2005; Johan, 2006; Malitch and Thalhammer, 2002; Tolstykh et al., 2004).

The PGM particles detected in the Elbe experienced multiple events of modifications after their formation. Postmagmatic, supergene processes often caused a heterogeneous distribution, oxidation and partly leaching of PGM grains, which is visualized by compositional differences between core and rim of individual grains (Fig. 3a, b). In general, the PGMs are of primary origin and formed during high-temperature processes as shown by other studies (Cabri et al., 2022a). The secondary processes caused compositional modifications of PGMs under supergene, low-temperature conditions, as similarly observed in laterites and near-surface PGE ore bodies (Aiglsperger et al., 2017; Bowles, 1986; Bowles et al., 2017; Junge et al., 2019; Korges et al., 2021; Locmelis et al., 2010; Oberthür, 2018; Oberthür et al., 2013b; Oberthür and Melcher, 2005; Zaccarini et al., 2013). The different mobility of metals results in a distinct compositional pattern and zoning of PGM grains. Fracturing during transportation allows infiltration of low-temperature meteoric waters and results in chemical modification within individual particles. The general shape and form of individual particles already argues for at least partly distal source areas due to longer transportation distances.

**Table 3.** Relative proportions of PGM investigated in the Elbe (this study), Rhine (Oberthür et al., 2016) and Danube (Dill et al., 2009): very abundant (+++), abundant (++) and present (+).

| PGM | Elbe | Rhine | Danube |
|---|---|---|---|
| Sperrylite | +++ | + | + |
| Pt–Fe | ++ | ++ | ++ |
| Os–Ir–Ru alloy | +++ | +++ | +++ |
| PGE sulfide | + | rare | rare |

### 5.3 Mineral compositions of Os–Ir–Ru alloys

Compositional variations were first shown on a ternary plot by Cabri (1972). The first nomenclature of Os–Ir–Ru alloys is still widely used (Harris and Cabri, 1973, 1991). Os–Ir–Ru alloys are chemically stable in supergene and fluvial environments due to their relatively high hardness with 6–7 on Mohs scale (Cabri, 2002; Cabri et al., 2022a). In general, Os–Ir–Ru alloys are almost absent in placers originating from ultramafic–mafic layered intrusions (Melcher et al., 2005; Oberthür et al., 2004, 2013a, 2014) or within near-surface oxidized ores overlying primary PGE deposits of ultramafic–mafic layered intrusions (Junge et al., 2019; Locmelis et al., 2010; Oberthür, 2018). However, dominance of Os–Ir–Ru alloys is frequently described in fluvial systems and placer deposits originating from ophiolites, Uralian–Alaskan-type complexes and laterites overlying ophiolites (Aiglsperger et al., 2017; Cabri et al., 2022a; González-Jiménez et al., 2009; Johann, 2002; Tolstykh et al., 2005; Weiser, 2002). Figure 6a shows the compositional variation of Os–Ir–Ru alloys from ophiolites (Hagen et al., 1990; Shcheka et al., 2004; Tol-

stykh et al., 2002b), Uralian–Alaskan-type complexes (Malitch et al., 2002; Tolstykh et al., 2002a, 2002b) and the Rhine (Oberthür et al., 2016). This shows that different source regions can be accounted for the Os–Ir–Ru alloys observed in the Elbe. See further discussion below.

In certain placer deposits, Os- and Ir-dominant alloys account for the most abundant PGM observed, such as in the Sisim watershed and Bolshoy Khailyk near Krasnoyarsk in Eastern Sayans, Russia (Barkov et al., 2018, 2019), and the Pados–Tundra ultramafic complex of the Kola Peninsula (Barkov et al., 2017). Zoning of Os–Ir–Ru alloys was observed in placer deposits worldwide, with typically a dominance by Os- and Ir-enriched rims (Barkov et al., 2018). In the Mesoarchean auriferous Witwatersrand conglomerate in South Africa, Os–Ir–Ru alloys with Ru contents below 20 atom % are the most common PGM (Feather, 1976). The PGM grains of Witwatersrand probably originate from mafic to ultramafic rocks of the Archean greenstone belts situated toward the north and northeast of the Witwatersrand Basin (Cousins, 1973; Feather, 1976). In placers of the island of Samar in the Philippines, Os–Ir–Ru alloys are characterized by highly variable composition covering nearly the entire ternary diagram as well as concentrations of Pt (Oberthür et al., 2017). Besides Os–Ir–Ru alloys, the PGM assemblages in placers of the island of Samar also consist of Pt–Fe alloys and laurite–erlichmanite, whereby Os–Ir–Ru and Pt–Fe alloys are the most frequent PGMs and are almost equally distributed (Oberthür et al., 2017). The source of the PGMs in the Samar placers is assumed to be ophiolites that are outcropping in the area (Oberthür et al., 2017). The similar PGM assemblage consisting of Ru–Os–Ir alloys and Pt–Fe alloys in the Elbe therefore argue for a similar origin.

A negative correlation between Ir and Os exists in the Sisim watershed, which was explained by a substitution of Os with Ir (Barkov et al., 2018). Similarly, the negative correlation between Ir and Os is observed for the particles from the Elbe (Fig. 7a). The Os–Ir–Ru alloys from the Rhine (Oberthür et al., 2016) and the Danube (Dill et al., 2009, 2010) are generally similar to those described here from the Elbe.

Native osmium has also been described in the Guli ultramafic massif in northern Siberia (Malich and Lopatin, 1997; Malitch et al., 2002; Merkle et al., 2012), in ophiolites and Uralian–Alaskan-type complexes (Garuti et al., 1999; González-Jiménez et al., 2009; Melcher et al., 1997; Zaccarini et al., 2005, 2018). Native osmium also been described from placer deposits such as the Witwatersrand in South Africa (Cousins, 1973; Feather, 1976; Malitch and Merkle, 2004; Merkle and Franklyn, 1999) and from various other placers worldwide (Barkov et al., 2018, 2019; Cabri et al., 1996; Stepanov et al., 2019; Weiser, 2002; Weiser and Bachmann, 1999).

### 5.4 Mineral compositions of PGE (Fe,Cu,Ni) alloys

PGE (Fe,Cu,Ni) alloys are typically described as stable minerals and are found in placer deposits worldwide (Barkov and Cabri, 2019; Cabri et al., 1996, 2022b; Melcher et al., 2005; Oberthür et al., 2004, 2013a, 2014; Shcheka et al., 2004; Weiser, 2002), European river systems (Dill et al., 2009; Oberthür et al., 2016) and laterites (Aiglsperger et al., 2015, 2017; Bowles et al., 2017). These alloys remain stable in near-surface oxidized ores overlying primary Ni–Cu–PGE mineralization (Junge et al., 2019; Locmelis et al., 2010; Oberthür, 2018). In general, a negative correlation between Pt and Fe is observed (Barkov and Cabri, 2019). Elevated concentrations of Ir (several wt %) are described from Uralian–Alaskan-type complexes as well as chromitite deposits, whereas Ir concentrations are low ($< 0.3$ wt %) from layered intrusions (Barkov and Cabri, 2019). The concentrations of the Pt–Fe alloys of this study range up to 9.67 atom % Ir (median 0.67 atom %), which are higher than the concentrations from layered intrusions. The concentrations therefore are rather similar to those published for Kondyor and Nizhny Tagil (Barkov and Cabri, 2019; Malitch and Thalhammer, 2002; Nekrasov et al., 2005). In this study, Pt–Fe alloys contained Pd concentrations of up to 46.38 atom %. The compositional variation of major and minor elements in PGE alloys is manifold, but major incorporations are Cu and Ni (Augé and Legendre, 1992; Barkov and Cabri, 2019). Plotting the range of data on PGE Fe demonstrates a miscibility gap between the ordered $Pt_3Fe$ structure and the disordered structure of native or ferroan platinum (Barkov and Cabri, 2019; Cabri et al., 2022b), which can be seen in Fig. 8c.

### 5.5 Mineral compositions of sperrylite

The mineral chemistry of sperrylite is generally homogenous. One sperrylite grain showed elevated concentrations of Pd (2.90 atom %), Rh (0.64 atom %) and Ir (1.07 atom %) but lower Pt values (28.11 atom %). This indicates that Pd, Rh and Ir can substitute for Pt in the sperrylite structure. High concentrations of Pd up to 10.36 atom % in sperrylite are reported by Gutierrez-Narbona et al. (2003). Similarly, S substitutes for As as shown by sperrylite with relatively lower As values but slightly higher S concentrations. Antimony shows similar but less pronounced behavior as S, as a few sperrylite grains had Sb values above the detection limit correlating with As values below the median values.

### 5.6 Mineralogical modification of platinum-group minerals

Comparing pristine and overlying near-surface oxidized PGE ores as well as studying alluvial and eluvial PGM showed that different stabilities of PGMs exist and therefore PGE phases react differently on weathering processes (Cabri et al., 2022a; Junge et al., 2019; Kraemer et al., 2015, 2017;

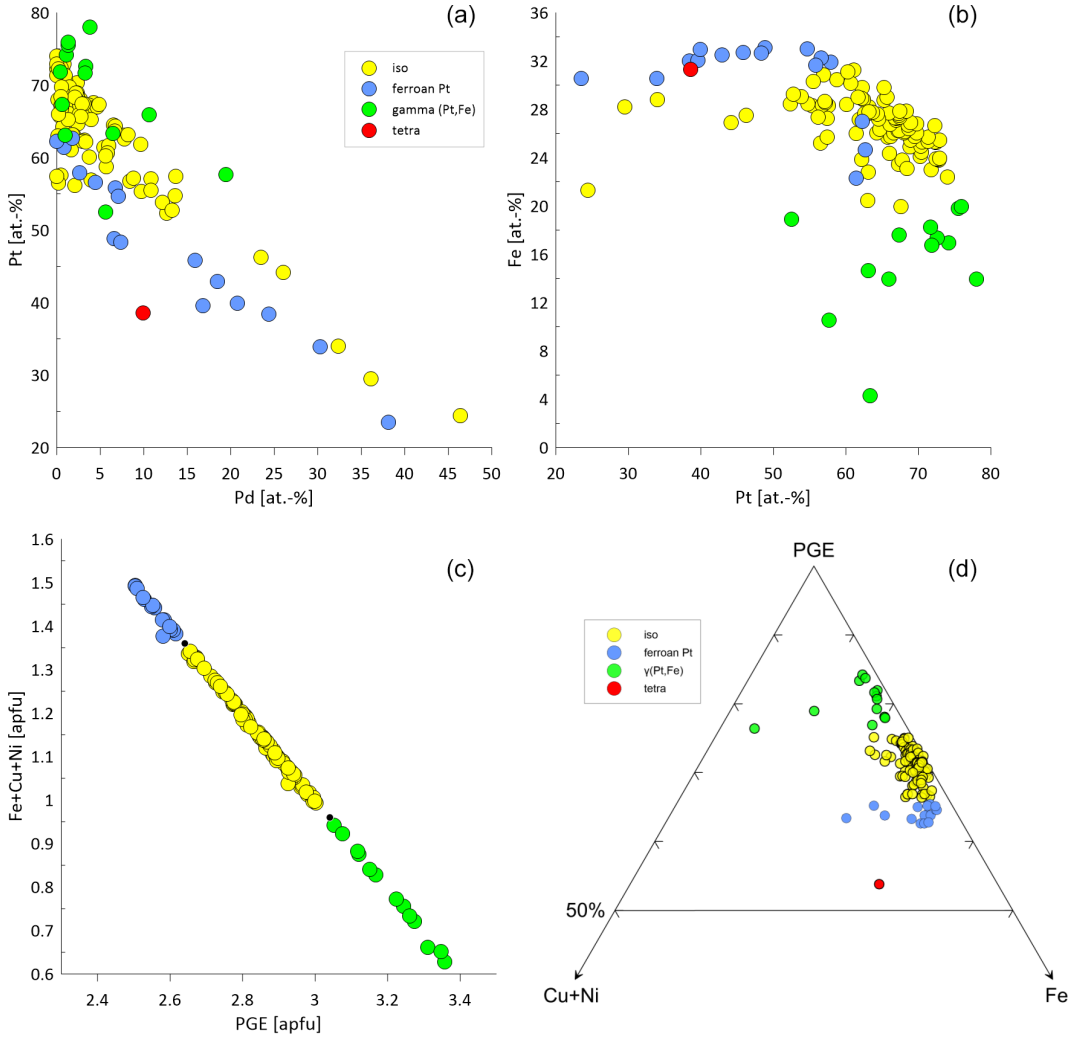


**Figure 8.** Compositional variability of the different Pt–Fe alloys classified as isoferroplatinum ($n = 93$), ferroan platinum ($n = 16$), $\gamma$(Pt,Fe) ($n = 14$) and tetraferroplatinum ($n = 1$). **(a)** Pt versus Pd in atom % showing a negative correlation. **(b)** Fe versus Pt visualizing the different compositional groups. **(c)** Good correlation between Fe + Cu + Ni [apfu] and PGE [apfu], showing corresponding element substitutions. The black dots correspond to the compositional boundaries as proposed by Cabri et al. (2022b). **(d)** Ternary plot of Fe–PGE–Cu + Ni to visualize the proportion of Fe in relation to Ni + Cu in PGE Fe alloys.

Locmelis et al., 2010; Oberthür, 2018; Oberthür et al., 2013a, 2014). This observation agrees with the findings of this study (Fig. 3a, b). The intergrowth of native platinum with sperrylite and the rim of platinum surrounding sperrylite argues for a late-stage modification of the sperrylite particle by releasing As. A surface coating of platinum on sperrylite grains was shown in supergene PGM deposits such as the Great Dyke, the Bushveld Complex and the Luanga Complex, and in the Rhine (Cabri et al., 2022a; Garuti and Zaccarini, 2021; Oberthür, 2018; Oberthür et al., 2016). Therefore, sperrylite can be altered to native Pt under non-tropical weathering and remains in situ, whereas arsenic is dispersed (Cabri et al., 2022a).

### 5.7 Source regions of PGM, Au and other heavy minerals

The geological drainage systems of the Elbe and Vltava cover various geological units of granitoids, gneisses, migmatites, ultramafic, gabbroic and sedimentary rocks. The large abundance of Os–Ir–Ru alloys as well as Pt–Fe alloys and sperrylite argues for ophiolites and Uralian–Alaskan-type complexes as the source regions. The geochemical character of Au and PGM rather requires ultramafic and gabbroic lithologies. Minor and smaller occurrences of gabbroic and ultramafic rocks are known from the drainage system (Ackerman et al., 2013; Fediuk, 2005; Járóka et al., 2019, 2021, 2023; Pašava et al., 2003, 2015) and are described below.

In general, Os–Ir–Ru alloys from the Elbe are well-rounded. In comparison, sperrylite and Pt–Fe alloys show rather euhedral shapes. This difference in the morphology of the PGM observed in the concentrate from the Elbe argues for different transportation distances and therefore different source areas.

The Ransko gabbro–peridotite massif (Fig. 1) hosts low-grade Ni–Cu–(PGE) ores, which are assumed to represent a liquid segregation style of mineralization (Ackerman et al., 2013; Pašava et al., 2003). The PGM distribution of the Ransko gabbro–peridotite massif mainly includes michenerite and froodite, i.e., PGE bismuthotellurides rather than Os–Ir–Ru and Pt–Fe alloys (Pašava et al., 2003). The Ransko gabbro–peridotite massif resembles Uralian–Alaskan-type intrusions (Pašava et al., 2003). Based on the geotectonic position and estimated age, the origin of the Ransko Massif is assumed to be formed during the post-Cadomian extension period, which was accompanied by the emplacement of numerous magmatic bodies in the Bohemian Massif (Pašava et al., 2003).

In addition to the Ransko gabbro–peridotite massif, in the drainage area of the Elbe various gabbroic and ultramafic intrusions and dikes hosting Ni–Cu–(PGE) sulfide mineralization and gold exist in Lusatia (Járóka et al., 2019, 2021, 2023; Sandmann and Gutzmer, 2014). At the Angstberg intrusion as well as the Sohland–Rožany Ni–Cu–(PGE) sulfide mineralization, PGMs are dominated by Pt–Pd bismuthotellurides and minor sperrylite (Járóka et al., 2019, 2021). This PGM assemblage is similar to the Ransko gabbro–peridotite massif. Similarly, at Kunratice in Bohemia (6 km southwest of Sohland–Rožany) the PGM assemblage is dominated by Pd bismuthotellurides and sperrylite (Sandmann and Gutzmer, 2014). However, studies of placers worldwide showed that Pt–Pd bismuthotellurides are relatively unstable and are therefore rarely observed in stream sediments (Oberthür, 2018; Oberthür et al., 2014). The different gabbroic dikes in the associated Sohland–Rožany Ni–Cu–(PGE) sulfide mineralization, Kunratice and the Angstberg intrusion can be at least the source region for the sperrylite and gold in this study. However, major occurrences of neither Pt–Fe alloys nor Os–Ir–Ru alloys were discovered in the region of the Lusatia.

In the Vestřev pyrope-rich garnet placer (Krkonoše Piedmont Basin) in the Bohemian Massif, Pt–Fe alloy particles are accompanied by Os–Ir–Ru minerals (native osmium, iridium, and ruthenium) with inclusions of Pt–Fe alloy and hongshiite (Pašava et al., 2015). The Os–Ir–Ru alloys are dominated by Ru, which is typical for ophiolites (Pašava et al., 2015). The PGM composition at the Vestřev pyrope-rich garnet placer therefore differs from Sohland–Rožany, Kunratice, Ransko and Angstberg.

In general, the stability of these PGE bismuthotellurides and Pt–Pd sulfides (such as cooperite/braggite) is generally low as they are very rare in placers and supergene environments associated with ultramafic rocks rich in PGE bismuthotellurides and Pt–Pd sulfides (Cabri et al., 2022a; Junge et al., 2019; Locmelis et al., 2010; Oberthür, 2018). For the Os–Ir–Ru alloys it was further shown that Os-rich Os–Ir–Ru alloys are more stable than Ru-rich Os–Ir–Ru alloys (Cabri et al., 2022a). The stability of sperrylite depends on chemical composition and climatic conditions as sperrylite particles with a platinum coating are observed in placers and in supergene deposits in rivers (Cabri et al., 2022a; Oberthür, 2018; Oberthür et al., 2016). Therefore, the large compositional variation of Os–Ir–Ru and Pt–Fe alloys argues for different source regions (Fig. 6b). However, a good correlation exists between the Os-poor Os–Ir–Ru alloys of this study and the Vestřev pyrope-rich garnet placer (Pašava et al., 2015). Similarly, inclusions of Pt–Fe alloys and Os–Ir–Ru alloys were observed in this study (Fig. 4c) and the Vestřev placer (Pašava et al., 2015), which argue for a source from the Vestřev placer as well. The alloys with higher Os concentrations should derive from Uralian–Alaskan types as these are typically rich in Os (Cabri et al., 2022a).

Platinum-group minerals, including Os–Ir–Ru alloys, are also observed from chondritic as well as iron meteorites which do have similarities to the observed composition of the Elbe (Bischoff et al., 2011; Geiger and Bischoff, 1995; Ma et al., 2014; Schulze et al., 1994). To some extent the observed PGMs can also be of extraterrestrial source as the accumulation of micrometeorites or meteorite dust has similar compositions of Os–Ir–Ru, and Pt–Fe alloys are described from meteorites (Baumgartner et al., 2017; Bischoff and Palme, 1987; Ma et al., 2014).

In the drainage area different source areas for cinnabar exist such as the Horní Luby ore district (Velebil and Zacharias, 2013) and the Jedová Hora (Hojdová et al., 2008; Pelcová et al., 2022; Sysalová et al., 2017). Gold occurrences are typically present in a larger range of rock types compared to PGM ranging from felsic, mafic to ultramafic rocks. Therefore, also different regions and lithologies might be the source for the gold grains shown in this study. Larger gold mineralization occurs within the Mokrsko-West gold deposit (Zachariáš, 2016; Zachariáš et al., 2014). The deposit is mainly hosted by tonalite of the Central Bohemian Plutonic Complex (Zachariáš et al., 2014). The total gold resource of the Mokrsko gold deposit is about 140 t (Morávek et al., 1989). However, the shape of the gold particles of the Elbe rather argues for short transportation distances as the gold particles are rather large and angled. Previous studies showed that the variation of gold particle size and morphology provides evidence for the transportation distances such as in the Lusatia gabbroic dikes and in other locations in Saxony close to Freiberg (Járóka et al., 2021, 2023; Lehmann, 2010). Gold particles with irregular shapes and with larger particle size in the centimeter-scale argue for short transportation distances, whereas rounded and smaller particles sizes experienced longer transportation in the river (Grant et al., 1991).

The cassiterite, ferberite, monazite, uraninite, tantalite, magnetite and zircon particles can be sourced from the Variscan granites, which are abundant in the drainage area of the Elbe and the Vltava.

## 6 Conclusions

Heavy mineral concentrates from the Elbe demonstrate that gold and PGM particles show different textures and morphology. The large quantities of PGMs analyzed by MLA demonstrate that Pt–Fe alloys and Os–Ir–Ru alloys are the most abundant PGMs in the Elbe. These PGM grains exist as monomineralic particles or as intergrowths with other minerals. Particles that contain measurable concentrations of Pt are typically Ir-rich, Ru-poor and Os-poor. The compositional variation of the Pt–Fe alloys showed substitution of Pt with the base metals Fe, Ni and Cu. Minor concentrations of Pd and Rh are detected in Pt–Fe. Gold particles are typically zoned consisting of Ag-poor rims and Ag-rich cores due to the greater mobility of Ag during weathering processes. Mercury-rich rims of the gold particles are the result of in situ amalgamation due to local mobilization of Hg from cinnabar. Similarly to gold, also PGM can be affected by alteration causing for example the modification of sperrylite resulting in a platinum-rich rim and a sperrylite core. Potential source regions for the PGM are the Vestřev and the gabbroic dike of the Lusatia block mineralization. These potential sources for the PGM sampled from the Elbe differ slightly in the mineralogical compositions. Therefore, a mix of different source regions can contribute to the heavy mineral concentrate observed in this study.

*Data availability.* Representative data shown in the figure are provided in the tables. The literature data of the figures are cited in the captions.

*Author contributions.* MJ and SG prepared the manuscript with contributions from HW. SG carried out the analytical part. HW did the upgrading of the mineral concentrates.

*Competing interests.* The contact author has declared that none of the authors has any competing interests.

*Disclaimer.* Publisher's note: Copernicus Publications remains neutral with regard to jurisdictional claims in published maps and institutional affiliations.

*Acknowledgements.* Polished sections were ably produced by Don Henry and Andreas Heiner from the BGR. Many thanks to Kai Lösel for providing the sample material. We thank Christian Wöhrl (BGR) for assisting with the electron microprobe work. Sadly, this year our colleague and co-author Herman Wotruba passed away and we keep him in our memory. We highly appreciate the constructive comments by Giorgio Garuti and one anonymous reviewer that sensibly improved the manuscript.

*Financial support.* This open-access publication was funded by Ludwig-Maximilians-Universität München.

*Review statement.* This paper was edited by Alessio Langella and reviewed by Giorgio Garuti and one anonymous referee.

## References

Ackerman, L., Pašava, J., and Erban, V.: Re-Os geochemistry and geochronology of the Ransko gabbro-peridotite massif, Bohemian Massif, Miner. Depos., 48, 799–804, https://doi.org/10.1007/s00126-013-0483-2, 2013.

Aiglsperger, T., Proenza, J. A., Zaccarini, F., Lewis, J. F., Garuti, G., Labrador, M., and Longo, F.: Platinum group minerals (PGM) in the Falcondo Ni-laterite deposit, Loma Caribe peridotite (Dominican Republic), Miner. Depos., 50, 105–123, https://doi.org/10.1007/s00126-014-0520-9, 2015.

Aiglsperger, T., Proenza, J. A., Font-Bardia, M., Baurier-Aymat, S., Galí, S., Lewis, J. F., and Longo, F.: Supergene neoformation of Pt-Ir-Fe-Ni alloys: multistage grains explain nugget formation in Ni-laterites, Miner. Depos., 52, 1069–1083, https://doi.org/10.1007/s00126-016-0692-6, 2017.

Albiez, G.: Neue Untersuchungenüber das Vorkommen von Rheingold, Berichte der Naturforschenden Gesellschaft zu Freibg. im Breisgau, 41, 179–204, 1951.

Augé, T. and Legendre, O.: Pt-Fe nuggets from alluvial deposits in eastern Madagascar, Can. Mineral., 30, 983–1004, 1992.

Bachmann, K., Frenzel, M., Krause, J., and Gutzmer, J.: Advanced Identification and Quantification of In-Bearing Minerals by Scanning Electron Microscope-Based Image Analysis, Microsc. Microanal., 23, 527–537, https://doi.org/10.1017/S1431927617000460, 2017.

Barkov, A. Y. and Cabri, L. J.: Variations of major and minor elements in Pt–Fe alloy minerals: A review and new observations, Minerals, 9, 1–15, https://doi.org/10.3390/min9010025, 2019.

Barkov, A. Y., Fleet, M. E., Nixon, G. T., and Levson, V. M.: Platinum-group minerals from five placer deposits in British Columbia, Canada, Can. Mineral., 43, 1687–1710, https://doi.org/10.2113/gscanmin.43.5.1687, 2005.

Barkov, A. Y., Nikiforov, A. A., Tolstykh, N. D., Shvedov, G. I., and Korolyuk, V. N.: Compounds of Ru–Se–S, alloys of Os–Ir, framboidal Ru nanophases, and laurite–clinochlore intergrowths in the Pados-Tundra complex, Kola Peninsula, Russia, Eur. J. Mineral., 29, 613–621, https://doi.org/10.1127/ejm/2017/0029-2666, 2017.

Barkov, A. Y., Shvedov, G. I., and Martin, R. F.: PGE-(REE-Ti)-rich micrometer-sized inclusions, mineral associations, compositional variations, and a potential lode source of platinum-group minerals in the sisim placer zone, eastern sayans, Russia, Minerals, 8, 1–19, https://doi.org/10.3390/min8050181, 2018.

Barkov, A. Y., Tamura, N., Shvedov, G. I., Stan, C. V., Ma, C., Winkler, B., and Martin, R. F.: Platiniferous tetra-auricupride: A case study from the bolshoy khailyk placer deposit, western Sayans, Russia, Minerals, 9, 1–10, https://doi.org/10.3390/min9030160, 2019.

Baumgartner, R., Fiorentini, M. L., Lorand, J.-P., Baratoux, D., Zaccarini, F., Ferriere, L., Prasek, M., and Sener, K.: The role of sulfides in the fractionation of highly siderophile and chalcophile elements during the formation of martian shergottite meteorites, Geochim. Cosmochim. Ac., 210, 1–24, 2017.

Baurier-Aymat, S., Jiménez-Franco, A., Roqué-Rosell, J., González-Jiménez, J. M., Gervilla, F., Proenza, J. A., Mendoza, J., and Nieto, F.: Nanoscale structure of zoned laurites from the Ojén Ultramafic Massif, Southern Spain, Minerals, 9, 1–18, https://doi.org/10.3390/min9050288, 2019.

Bischoff, A. and Palme, H.: Composition and mineralogy of refractory-metal-rich assemblages from a Ca,Al-rich inclusion in the Allende meteorite, Geochim. Cosmochim. Ac., 51, 2733–2748, https://doi.org/10.1016/0016-7037(87)90153-0, 1987.

Bischoff, A., Vogel, N., and Roszjar, J.: The Rumuruti chondrite group, Chem. Erde-Geochem., 71, 101–133, https://doi.org/10.1016/j.chemer.2011.02.005, 2011.

Bowell, R. J.: Supergene gold mineralogy at Ashanti, Ghana: Implications for the supergene behaviour of gold, Mineral. Mag., 56, 545–560, https://doi.org/10.1180/minmag.1992.056.385.10, 1992.

Bowles, J. F. W.: The development of platinum-group minerals in laterites, Econ. Geol., 81, 1278–1285, https://doi.org/10.2113/gsecongeo.81.5.1278, 1986.

Bowles, J. F. W., Suárez, S., Prichard, H. M., and Fisher, P. C.: Weathering of PGE sulfides and Pt–Fe alloys in the Freetown Layered Complex, Sierra Leone, Miner. Depos., 52, 1127–1144, https://doi.org/10.1007/s00126-016-0706-4, 2017.

Cabri, L. J.: The mineralogy of the platinum-group elements, Miner. Sci. Eng., 4, 3–29, 1972.

Cabri, L. J.: The Platinum-Group Minerals, in: The Geology, Geochemistry, Mineralogy and Mineral Beneficiation of Platinum-group Elements, edited by: Cabri, L. J., CIM Special, Canadian Institute of Mining, Metallurgy and Petroleum, Montreal, 13–129, ISBN: 9781894475273, 2002.

Cabri, L. J. and Feather, C. E.: Platinum-iron alloys: A nomenclature based on a study of natural and synthetic alloys, Can. Mineral., 13, 117–126, 1975.

Cabri, L. J. and Genkin, A. D.: Re-examination of Pt-Fe alloy from lode and placer deposits, Urals, Can. Mineral., 29, 419–425, 1991.

Cabri, L. J. and Harris, D. C.: Zoning in Os-Ir alloys and the relation of the geological and tectonic environment of the source rocks to the bulk Pt : Pt + Ir + Os ratio for placers, Can. Mineral., 13, 266–274, 1975.

Cabri, L. J., Harris, D. C., and Weiser, T. W.: Mineralogy and distribution of platinum-group mineral (PGM) placer deposits of the world, Explor. Min. Geol., 5, 73–167, 1996.

Cabri, L. J., Oberthür, T., and Keays, R.: Origin and depositional history of platinum-group minerals in placers – A critical review of facts and fiction, Ore Geol. Rev., 144, 104733, https://doi.org/10.1016/j.oregeorev.2022.104733, 2022a.

Cabri, L. J., Oberthür, T., and Schumann, D.: The Mineralogy of Pt-Fe alloys and phase relations in the Pt–Fe binary system, Can. Mineral., 60, 331–339, 2022b.

Cawthorn, R. G.: The discovery of the platiniferous Merensky Reef in 1924, South Afr. J. Geol., 102, 178–183, 1999.

Chapman, R. J., Leake, R. C., Bond, D. P. G., Stedra, V., and Fairgrieve, B.: Chemical and mineralogical signatures of gold formed in oxidizing chloride hydrothermal systems and their significance within populations of placer gold grains collected during reconnaissance, Econ. Geol., 104, 563–585, 2009.

Chapman, R. J., Mortensen, J. K., Crawford, E. C., and Lebarge, W.: Microchemical studies of placer and lode gold in the Klondike District, Yukon, Canada: 1. Evidence for a small, gold-rich, orogenic hydrothermal system in the Bonanza and Eldorado Creek area, Econ. Geol., 105, 1369–1392, 2010.

Chapman, R. J., Mileham, T., Allan, M. M., and Mortensen, J. K.: A distinctive Pd-Hg signature in detrital gold derived from alkalic Cu-Au porphyry systems, Ore Geol. Rev., 83, 84–102, 2017.

Chapman, R. J., Banks, D. A., Styles, M. T., Walshaw, R. D., Piazolo, S., Morgan, D. J., Spence-Jones, C. P., Matthews, T. J., and Borovinskaya, O.: Chemical and physical heterogeneity within native gold: implications for the design of gold particle studies, Mineral. Depos., 56, 1563–1588, 2021.

Cousins, C. A.: Platinoids of the Witwatersrand system, J. South Afr. Inst. Min. Metall., 73, 184–199, 1973.

Desborough, G. A.: Silver depletion indicated by microanalysis of gold from placer occurrences, Western United State, Econ. Geol., 65, 304–311, https://doi.org/10.2113/gsecongeo.65.3.304, 1970.

Dijkstra, A. H., Dale, C. W., Oberthür, T., Nowell, G. M., and Graham Pearson, D.: Osmium isotope compositions of detrital Os-rich alloys from the Rhine River provide evidence for a global late Mesoproterozoic mantle depletion event, Earth Planet. Sc. Lett., 452, 115–122, https://doi.org/10.1016/j.epsl.2016.07.047, 2016.

Dill, H. G.: Grain morphology of heavy minerals from marine and continental placer deposits, with special reference to Fe–Ti oxides, Sediment. Geol., 198, 1–27, 2007.

Dill, H. G., Klosa, D., Steyer, G., and Fuessle, M.: Schwermineraluntersuchungen an Palladium-, Iridium- und Osmium-Minerale führenden Goldseifen aus Niederbayern, Deutschland, Z. Dtsch. Ges. Geowiss., 158, 1005–1010, 2007.

Dill, H. G., Klosa, D., and Steyer, G.: The "Donauplatin": Source rock analysis and origin of a distal fluvial Au-PGE placer in Central Europe, Mineral. Petrol., 96, 141–161, https://doi.org/10.1007/s00710-009-0060-7, 2009.

Dill, H. G., Weber, B., and Steyer, G.: Morphological studies of PGM grains in alluvial-fluvial placer deposits from the Bayerischer Wald, SE Germany: Hollingworthite and ferroan platinum, Neues Jahrb. Mineral. Abhandlungen, 187, 101–110, https://doi.org/10.1127/0077-7757/2010/0155, 2010.

Economou-Eliopoulos, M.: Platinum-group element distribution in chromite ores from ophiolite complexes: Implications for their exploration, Ore Geol. Rev., 11, 363–381, https://doi.org/10.1016/S0169-1368(96)00008-X, 1996.

Elsner, H.: Goldgewinnung in Deutschland – Historie und Potenzial, Commodity Top News, Vol. 30, 1–10, Bundesanstalt für Geowissenschaften und Rohstoffe, https://www.bgr.bund.de/DE/Gemeinsames/Produkte/Downloads/Commodity_Top_News/

Rohstoffwirtschaft/30_gold.pdf?__blob=publicationFile&v=3 (last access: 3 July 2023), 2009.

Fairbrother, L., Brugger, J., Shapter, J., Laird, J. S., Southam, G., and Reith, F.: Supergene gold transformation: Biogenic secondary and nano-particulate gold from arid Australia, Chem. Geol., 320/321, 17–31, https://doi.org/10.1016/j.chemgeo.2012.05.025, 2012.

Fandrich, R., Gu, Y., Burrows, D., and Moeller, K.: Modern SEM-based mineral liberation analysis, Int. J. Miner. Process., 84, 310–320, https://doi.org/10.1016/j.minpro.2006.07.018, 2007.

Feather, C. E.: Mineralogy of platinum-group minerals in the Witwatersrand, South Africa, Econ. Geol., 71, 1399–1428, https://doi.org/10.2113/gsecongeo.71.7.1399, 1976.

Fediuk, F.: The Lower Vltava River Pluton: A semi-hidden intrusive complex in Neoproterozoic at the northern outskirts of Prague, Central Bohemia, J. Czech Geol. Soc., 50, 71–80, https://doi.org/10.3190/jcgs.978, 2005.

Garuti, G. and Zaccarini, F.: Naldrettite (Pd2Sb): a new find in Brazil and comparison with worldwide occurrences, Can. Mineral., 59, 1801–1820, 2021.

Garuti, G., Fershtater, G., Bea, F., Montero, P., Pushkarev, E. V., and Zaccarini, F.: Platinum-group elements as petrological indicators in mafic-ultramafic complexes of the central and southern Urals: Preliminary results, Tectonophysics, 276, 181–194, https://doi.org/10.1016/S0040-1951(97)00050-4, 1997.

Garuti, G., Zaccarini, F., Moloshag, V., and Alimov, V.: Platinum-group minerals as indicators of sulfur fugacity in ophiolitic upper mantle: An example from chromitites of the Ray-Iz ultramafic complex, Polar Urals, Russia, Can. Mineral., 37, 1099–1115, 1999.

Geiger, T. and Bischoff, A.: Formation of opaque minerals in CK chondrites, Planet. Space Sci., 43, 485–498, https://doi.org/10.1016/0032-0633(94)00173-O, 1995.

Goldenberg, G.: Platinmetalle im Rheinsand, Der Aufschluss, 39, 57–64, 1988.

González-Jiménez, J. M., and Reich, M.: An overview of the platinum-group element nanoparticles in mantle-hosted chromite deposits, Ore Geol. Rev., 81, 1236–1248, https://doi.org/10.1016/j.oregeorev.2016.06.022, 2017.

González-Jiménez, J. M., Gervilla, F., Proenza, J. A., Augé, T., and Kerestedjian, T.: Distribution of platinum-group minerals in ophiolitic chromitites, Trans. Inst. Min. Metall. Sect. B, 118, 101–110, https://doi.org/10.1179/174327509X12550990457924, 2009.

González-Jiménez, J. M., Griffin, W. L., Gervilla, F., Proenza, J. A., O'Reilly, S. Y., and Pearson, N. J.: Chromitites in ophiolites: How, where, when, why?, Part I. A review and new ideas on the origin and significance of platinum-group minerals, Lithos, 189, 127–139, https://doi.org/10.1016/j.lithos.2013.06.016, 2014a.

González-Jiménez, J. M., Griffin, W. L., Proenza, J. A., Gervilla, F., O'Reilly, S. Y., Akbulut, M., Pearson, N. J., and Arai, S.: Chromitites in ophiolites: How, where, when, why?, Part II. The crystallization of chromitites, Lithos, 190/191, 140–158, https://doi.org/10.1016/j.lithos.2013.09.008, 2014b.

González-Jiménez, J. M., Deditius, A., Gervilla, F., Reich, M., Suvorova, A., Roberts, M. P., Roqué, J., and Proenza, J. A.: Nanoscale partitioning of Ru, Ir, and Pt in base-metal sulfides from the Caridad chromite deposit, Cuba, Am. Mineral., 103, 1208–1220, https://doi.org/10.2138/am-2018-6424, 2018.

González-Jiménez, J. M., Roqué-Rosell, J., Jiménez-Franco, A., Tassara, S., Nieto, F., Gervilla, F., Baurier, S., Proenza, J. A., Saunders, E., Deditius, A. P., Schilling, M., and Corgne, A.: Magmatic platinum nanoparticles in metasomatic silicate glasses and sulfides from Patagonian mantle xenoliths, Contrib. Mineral. Petrol., 174, 1–8, https://doi.org/10.1007/s00410-019-1583-5, 2019.

González-Jiménez, J. M., Tassara, S., Schettino, E., Roqué-Rosell, J., Farré-de-Pablo, J., Saunders, J. E., Deditius, A. P., Colás, V., Rovira-Medina, J. J., M.G., D., Schilling, M., Jimenez-Franco, A., Marchesi, C., Nieto, F., J.A., P., and Gervilla, F.: Mineralogy of the HSE in the subcontinental lithospheric mantle – An interpretive review, Lithos, 372/373, 1–20, 2020.

Grant, A. H., Lavin, O. P., and Nichol, I.: The morphology and chemistry of transported gold grains as an exploration tool, J. Geochemical Explor., 40, 73–94, 1991.

Groen, J. C., Craig, J. R., and Rimstidt, J. D.: Gold-rich rim formation on electrum grains in placers, Can. Mineral., 28, 207–228, 1990.

Gu, Y.: Automated Scanning Electron Microscope Based Mineral Liberation Analysis An Introduction to JKMRC/FEI Mineral Liberation Analyser, J. Miner. Mater. Charact. Eng., 2, 33–41, https://doi.org/10.4236/jmmce.2003.21003, 2003.

Gutierrez-Narbona, R., Jean-Pierre, L., Gervilla, F., and Gros, M.: New data on base metal mineralogy and platinumgroup minerals in the Ojen chromitites (Serrania de Ronda, Betic Cordillera, southern Spain), Neues Jahrb. Mineral. Abhandl., 179, 143–173, 2003.

Gutzmer, J., Richter, L., Hennig, S., Petermann, T., and Lehmann, U.: Gold in sächsischen Kies- und Sandlagerstätten, Sächsisches Landesamt für Umwelt, Landwirt. Geol., 12, urn:nbn:de:bsz:14-qucosa-119258, 2013.

Hagen, D., Weiser, T., and Iltay, T.: Platinum-group minerals in Quaternary gold placers in the upper Chindwin area of northern Burma, Mineral. Petrol., 42, 265–286, 1990.

Hallbauer, D. K. and Utter, T.: Geochemical and morphological characteristics of gold particles from recent river deposits and the fossil placers of the Witwatersrand, Miner. Depos., 42, 293–306, 1977.

Harris, D. and Cabri, L. C.: Nomenclature of Platinum – Group – Element Alloys: Review and Revision, Can. Mineral., 29, 231–237, 1991.

Harris, D. C. and Cabri, L. J.: The nomenclature of the natural alloys of osmium, iridium, and ruthenium based on new compositional data of alloys from worldwide occurrences, Can. Mineral., 12, 104–112, 1973.

Hejzlar, J., Vyhnalek, V., Kopacek, J., and Duras, J.: Sources and transport of phosphorus in the Vltava river basin (Czech Republic), Water Sci. Technol., 33, 137–144, 1996.

Helmy, H. M., Ballhaus, C., and Wirth, R.: Noble metal nanoclusters and nanoparticles precede mineral formation in magmatic sulphide melts, Nat. Commun., 4, 1–7, 2013.

Hladil, J., Patočka, F., Kachlík, V., Melichar, R., and Hubačík, M.: Metamorphosed carbonates of Krkonoše Mountains and Paleozoic evolution of Sudetic terranes (NE Bohemia, Czech Republic), Geol. Carpath., 54, 281–297, 2003.

Hofmann, F.: Untersuchungen über den Goldgehalt der Oberen Marinen Molasse und des Stubensandsteins in der Gegend von Schaffhausen, Schweiz. Miner. Petrog., 45, 131–137, 1965.

Hofmann, M., Voigt, T., Bittner, L., Gärtner, A., Zieger, J., and Linnemann, U.: Reworked Middle Jurassic sandstones as a marker for Upper Cretaceous basin inversion in Central Europe – a case study for the U–Pb detrital zircon record of the Upper Cretaceous Schmilka section and their implication for the sedimentary cover of the Lausitz, Int. J. Earth Sci., 107, 913–932, 2018.

Hojdová, M., Navrátil, T., and Rohovec, J.: Distribution and speciation of mercury in mine waste dumps, Bull. Environ. Contam. Toxicol., 80, 237–241, 2008.

Holley, E. A., McQuillan, A. J., Craw, D., Kim, J. P., and Sander, S. G.: Mercury mobilization by oxidative dissolution of cinnabar ($\alpha$-HgS) and metacinnabar ($\beta$-HgS), Chem. Geol., 240, 313–325, 2007.

Janoušek, V., Rogers, G., and Bowes, D. R.: Sr-Nd isotopic constraints on the petrogenesis of the Central Bohemian Pluton, Czech Republic, Geol. Rundschau, 84, 520–534, https://doi.org/10.1007/BF00284518, 1995.

Járóka, T., Seifert, T., Pfänder, J. A., Staude, S., Seibel, H. V. L., Krause, J., and Bauer, M. E.: Geology, sulfide mineralogy and petrogenesis of the Angstberg Ni-Cu-(PGE)sulfide mineralization (Lausitz Block, Bohemian Massif, Germany): A potential Ni-Cu exploration target in Central Europe?, Ore Geol. Rev., 110, 1–25, https://doi.org/10.1016/j.oregeorev.2019.05.010, 2019.

Járóka, T., Staude, S., Seifert, T., Pfänder, J. A., Bauer, M. E., Krause, J., and Schulz, B.: Mineralogical and geochemical constraints on the origin of the Sohland-Rožany Ni-Cu-(PGE) sulfide mineralization (Lausitz Block, Bohemian Massif, Germany/Czech Republic), Ore Geol. Rev., 133, 104055, https://doi.org/10.1016/j.oregeorev.2021.104055, 2021.

Járóka, T., Pfänder, J. A., Seifert, T., Hauff, F., Sperner, B., Staude, S., Stephan, T., and Schulz, B.: Age and petrogenesis of Ni-Cu-(PGE) sulfide-bearing gabbroic intrusions in the Lausitz Block, northern Bohemian Massif (Germany/Czech Republic), Lithos, 444–445, 107090, https://doi.org/10.1016/j.lithos.2023.107090, 2023.

Johan, Z.: Platinum-group minerals from placers related to the Nizhni Tagil (Middle Urals, Russia) Uralian-Alaskan-type ultramafic complex: Ore-mineralogy and study of silicate inclusions in (Pt, Fe) alloys, Mineral. Petrol., 87, 1–30, https://doi.org/10.1007/s00710-005-0117-1, 2006.

Johann, Z.: Alaskan-type intrusive complexes and their PGE mineralization, in: The geology, geochemistry, mineralogy and mineral beneficiation of the platinum-group elements, edited by: Cabri, L. J., Canadian Institute of Mining, Metallurgy and Petroleum, Montreal, CIM Special, Vol. 54, 669–719, 424 pp., ISBN: 9781894475273, 2002.

Junge, M., Oberthür, T., and Melcher, F.: Cryptic variation of chromite chemistry, platinum group element and platinum group mineral distribution in the UG-2 chromitite: An example from the karee mine, western Bushveld complex, South Africa, Econ. Geol., 109, 795–810, https://doi.org/10.2113/econgeo.109.3.795, 2014.

Junge, M., Wirth, R., Oberthür, T., Melcher, F., and Schreiber, A.: Mineralogical siting of platinum-group elements in pentlandite from the Bushveld Complex, South Africa, Miner. Depos., 50, 41–54, https://doi.org/10.1007/s00126-014-0561-0, 2015.

Junge, M., Oberthür, T., Kraemer, D., Melcher, F., Piña, R., Derrey, I. T., Manyeruke, T., and Strauss, H.: Distribution of platinum-group elements in pristine and near-surface oxidized Platreef ore and the variation along strike, northern Bushveld Complex, South Africa, Miner. Depos., 54, 885–912, https://doi.org/10.1007/s00126-018-0848-7, 2019.

Kaufmann, H. and Lehmann, U.: Kiessandlagerstätten in Nordwest-Sachsen: Lieferanten wichtiger Massen-Rohstoffe (und hochwertiger Edelmetalle: Gold, Platinoide?), in: GeoTop 2016 Kultur.Wert.Stein Verantwortung und Chancen für Geoparks, edited by: Heß, H., Rascher, V., and Zellmer, J., Schriftenreihe der Deutschen Gesellschaft für Geowissenschaften, Heft 88, 139–149, 2016.

Kinnunen, K. A.: Mercury-rich coating on some gold nuggets from Ivalojoki placers, northern Finland, Spec. Pap. Surv. Finl., 36, 29–34, 2003.

Kirchheimer, F.: Über das Rheingold [Gold from the rhine], Aufschluss, 20, 184–187, 1969.

Knab, M., Hoffmann, V., Petrovský, E., Kapička, A., Jordanova, N., and Appel, E.: Surveying the anthropogenic impact of the Moldau river sediments and nearby soils using magnetic susceptibility, Environ. Geol., 49, 527–535, https://doi.org/10.1007/s00254-005-0080-5, 2006.

Knight, J. B., Mortensen, J. K., and Morison, S. R.: Lode and placer gold composition in the Klondike District, Yukon Territory, Canada; implications for the nature and genesis of Klondike placer and lode gold deposits, Econ. Geol., 94, 649–664, 1999.

Korges, M., Junge, M., Borg, G., and Oberthür, T.: Supergene mobilization and redistribution of platinum-group elements in the Merensky Reef, eastern Bushveld Complex, South Africa, Can. Mineral., 59, 1381–1396, 2021.

Kraemer, D., Junge, M., Oberthür, T., and Bau, M.: Improving recoveries of platinum and palladium from oxidized Platinum-Group Element ores of the Great Dyke, Zimbabwe, using the biogenic siderophore Desferrioxamine B, Hydrometallurgy, 152, 169–177, https://doi.org/10.1016/j.hydromet.2015.01.002, 2015.

Kraemer, D., Junge, M., and Bau, M.: Oxidized Ores as Future Resource for Platinum Group Metals: Current State of Research, Chemie-Ingenieur-Technik, 89, 53–63, https://doi.org/10.1002/cite.201600092, 2017.

Larizzatti, J. H., Oliveira, S. M. B., and Butt, C. R. M.: Morphology and composition of gold in a lateritic profile, Fazenda Pison "Garimpo", Amazon, Brazil, J. South Am. Earth Sci., 25, 359–376, https://doi.org/10.1016/j.jsames.2007.06.002, 2008.

Lehmann, U.: Gold in sächsischen Kiessandlagerstätten, Glückauf, 146, 560–564, 2010.

Lehrberger, G.: Gold in Bayern Vorkommen am Westrand der Böhmischen Masse, Bayerisches Geologisches Landesamt, Geologica Bavarica Band 102, 1997.

Locmelis, M., Melcher, F., and Oberthür, T.: Platinum-group element distribution in the oxidized Main Sulfide Zone, Great Dyke, Zimbabwe, Miner. Depos., 45, 93–109, https://doi.org/10.1007/s00126-009-0258-y, 2010.

Ma, C., Beckett, J. R., and Rossman, G. R.: Allendeite ($Sc_4Zr_3O_{12}$) and hexamolybdenum (Mo, Ru, Fe), two new minerals from an ultrarefractory inclusion from the Allende meteorite, Am. Mineral., 99, 654–666, https://doi.org/10.2138/am.2014.4667, 2014.

Malich, K. N. and Lopatin, G. G.: New data on the metallogeny of the unique gulin klinopyroxenite-dunite massif (northern Siberia, Russia), Geol. Ore Depos., 39, 209–218, 1997.

Malitch, K. N. and Merkle, R. K. W.: Ru-Os-Ir-Pt and Pt-Fe alloys from the evander goldfield, Witwatersrand Basin, South Africa: Detrital origin inferred from compositional and osmium-isotope data, Can. Mineral., 42, 631–650, https://doi.org/10.2113/gscanmin.42.2.631, 2004.

Malitch, K. N. and Thalhammer, O. A. R.: Pt-Fe nuggets derived from clinopyroxenite-dunite massifs, Russia: A structural, compositional and osmium-isotope study, Can. Mineral., 40, 395–418, https://doi.org/10.2113/gscanmin.40.2.395, 2002.

Malitch, K. N., Augé, T., Badanina, I. Y., Goncharov, M. M., Junk, S. A., and Pernicka, E.: Os-rich nuggets from Au-PGE placers of the Maimecha-Kotui Province, Russia: A multi-disciplinary study, Mineral. Petrol., 76, 121–148, https://doi.org/10.1007/s007100200035, 2002.

Mann, A. W.: Mobility of gold and silver in lateritic weathering profiles: some observations from Western Australia., Econ. Geol., 79, 38–49, https://doi.org/10.2113/gsecongeo.79.1.38, 1984.

Melcher, F., Grum, W., Simon, G., Thalhammer, T. V., and Stumpfl, E. F.: Petrogenesis of the ophiolitic giant chromite deposits of Kempirsai, Kazakhstan: A study of solid and fluid inclusions in chromite, J. Petrol., 38, 1419–1458, https://doi.org/10.1093/petroj/38.10.1419, 1997.

Melcher, F., Oberthür, T., and Lodziak, J.: Modification of detrital platinum-group minerals from the Eastern Bushveld Complex, South Africa, Can. Mineral., 43, 1711–1734, https://doi.org/10.2113/gscanmin.43.5.1711, 2005.

Merensky, H.: The various platinum occurrences on the farm Maandagshoek No. 148, Archives of the Merensky Trust, Duivelskloof, South Africa, Lydenburg Platinum Syndicate, 1924.

Merensky, H.: Die neuentdeckten Platinfelder im mittleren Transvaal und ihre wirtschaftliche Bedeutung, Z. Dtsch. Ges. Geowiss., 78, 296–314, 1926.

Merkle, R. K. W. and Franklyn, C. B.: Milli-PIXE determination of trace elements in osmium-rich platinum-group minerals from the Witwatersrand basin, South Africa, Nucl. Instruments Methods Phys. Res. Sect. B, 158, 556–561, https://doi.org/10.1016/S0168-583X(99)00499-1, 1999.

Merkle, R. K. W., Malitch, K. N., Gräser, P. P. H., and Badanina, I. Y.: Native osmium from the Guli Massif, Northern Siberia, Russia, Mineral. Petrol., 104, 115–127, https://doi.org/10.1007/s00710-011-0173-7, 2012.

Miller, J. W., Callahan, J. E., and Craig, J. R.: Mercury interactions in a simulated gold placer, Appl. Geochem., 17, 21–28, 2002.

Moles, N. R., Chapman, R. J., and Warner, R. B.: The significance of copper concentrations in natural gold alloy for reconnaissance exploration and understanding gold-depositing hydrothermal systems, Geochem. Explor. Environ. Anal., 13, 115–130, 2013.

Morávek, P., Janatka, J., Pertoldová, J., Straka, E., Ďurišová, J., and Pudilová, M.: The Mokrsko gold deposit – the largest gold deposit in the Bohemian Massif, Czechoslovakia, in: The Geology of Gold Deposits: The Perspective in 1988, Economic Geology Publ. Co, edited by: Keays, Reid R., Ramsay, W. R. H., and Groves, D. I., ISBN-10: 9990608091, 1989.

Nekrasov, I. Y., Lennikov, A. M., Zalishchak, B. L., Oktyabrsky, R. A., Ivanov, V. V., Sapin, V. I., and Taskaev, V. I.: Compositional variations in platinum-group minerals and gold, Konder alkaline-ultrabasic massif, Aldan Shield, Russia, Can. Mineral., 43, 637–654, 2005.

O'Driscoll, B. and González-Jiménez, J. M.: Petrogenesis of the platinum-group minerals, Rev. Mineral. Geochem., 81, 489–578, 2015.

Oberthür, T.: Platinum-group element mineralization of the Main Sulfide Zone, Great Dyke, Zimbabwe, in: Reviews in Economic Geology, Vol. 17, Magmatic Ni-Cu and PGE Deposits: Geology, Geochemistry, and Genesis, Society of Economic Geologist, edited by: Li, C. and Ripley, E. M., 29–349, https://doi.org/10.5382/Rev.17, 2011.

Oberthür, T.: The fate of platinum-group minerals in the exogenic environment – from sulfide ores via oxidized ores into placers: Case studies bushveld complex, South Africa, and Great Dyke, Zimbabwe, Minerals, 8, 1–28, https://doi.org/10.3390/min8120581, 2018.

Oberthür, T. and Melcher, F.: Behaviour of PGE and PGM in the supergene environment: a case study of persistence and redistribution in the Main Sulphide Zone of the Great Dyke, Zimbabwe, in: Exploration for Platinum – Group Element Deposits. Short Course 35, Mineralogical Association of Canada, edited by: Mungall, J. E., 97–111, ISBN: 0-921294-35-2, 2005.

Oberthür, T. and Saager, R.: Silver and Mercury in Gold Particles from the Proterozoic Witwatersrand Placer Deposits of South Africa: Metallogenic and Geochemical Implications, Econ. Geol., 81, 20–31, 1986.

Oberthür, T., Melcher, F., Gast, L., Wöhrl, C., and Lodziak, J.: Detrital platinum-group minerals in rivers draining the eastern Bushveld complex, South Africa, Can. Mineral., 42, 563–582, https://doi.org/10.2113/gscanmin.42.2.563, 2004.

Oberthür, T., Weiser, T. W., Melcher, F., Gast, L., and Wöhrl, .: Detrital platinum-group minerals in rivers draining the Great Dyke, Zimbabwe, Can. Mineral., 51, 197–222, https://doi.org/10.3749/canmin.51.2.197, 2013a.

Oberthür, T., Melcher, F., Buchholz, P., and Locmelis, M.: The oxidized ores of the Main Sulphide Zone, Great Dyke, Zimbabwe: Turning resources into minable reserves-mineralogy is the key, J. South. African Inst. Min. Metall., 113, 191–201, 2013b.

Oberthür, T., Weiser, T. W., and Melcher, F.: Alluvial and Eluvial Platinum-Group Minerals From the Bushveld Complex, South Africa, South Afr. J. Geol., 117, 255–274, https://doi.org/10.2113/gssajg.117.2.255, 2014.

Oberthür, T., Melcher, F., Goldmann, S., Wotruba, H., Gerdes, A., Dijkstra, A., and Dale, C. W.: Mineralogy and mineral chemistry of detrital heavy minerals from the Rhine River in Germany as evidence to their provenance, sedimentary and depositional history: focus on platinum-group minerals and remarks on cassiterite, columbite-group minerals and ur, Int. J. Earth Sci., 105, 637–657, https://doi.org/10.1007/s00531-015-1181-3, 2016.

Oberthür, T., Melcher, F., and Weiser, T. W.: Detrital platinum-group minerals and gold in placers of Southeastern Samar Island, Philippines, Can. Mineral., 55, 45–62, https://doi.org/10.3749/canmin.1600048, 2017.

Okamoto, H., Chakrabartl, D. J., Laughlin, D. E., and Masselski, T. B.: The Au-Cu (gold-copper) system, J. Phase Equilib., 8, 454–474, 1987.

Okrugin, A.: Origin of platinum-group minerals from dispersed elements to nuggets in mafic-ultramafic intrusive rocks, Can. Mineral., 49, 1397–2141, 2011.

Osbahr, I., Krause, J., Bachmann, K., and Gutzmer, J.: Efficient and Accurate Identification of Platinum-Group Minerals by a Com-

bination of Mineral Liberation and Electron Probe Microanalysis with a New Approach to the Offline Overlap Correction of Platinum-Group Element Concentrations, Microsc. Microanal., 21, 1080–1095, https://doi.org/10.1017/S1431927615000719, 2015.

Pašava, J., Vavřín, I., Frýda, J., Janoušek, V., and Jelínek, E.: Geochemistry and mineralogy of Platinum-group elements in the Ransko gabbro-peridotite massif, Bohemian Massif (Czech Republic), Miner. Depos., 38, 298–311, https://doi.org/10.1007/s00126-002-0343-y, 2003.

Pašava, J., Malec, J., Griffin, W. L., and González-Jiménez, J. M.: Re-Os isotopic constraints on the source of platinum-group minerals (PGMs) from the Vestřev pyrope-rich garnet placer deposit, Bohemian Massif, Ore Geol. Rev., 68, 117–126, https://doi.org/10.1016/j.oregeorev.2015.01.013, 2015.

Pelcová, P., Grmela, J., Ridošková, A., Kopp, R., Hrůzová, M., and Malý, O.: Trophic distribution of mercury from an abandoned cinnabar mine within the Záskalská reservoir ecosystem (Czech Republic), Environ. Sci. Pollut. Res., 29, 61383–61396, 2022.

Pfeiffer, W. C., de Lacerda, L. D., Malm, O., Souza, C. M. M., da Silveira, E. G., and Bastos, W. R.: Mercury concentrations in inland waters of gold-mining areas in Rondônia, Brazil, Sci. Total Environ., 87, 233–240, 1989.

Pfeiffer, W. C., Lacerda, L. D., Salomons, W., and Malm, O.: Environmental fate of mercury from gold mining in the Brazilian Amazon, Environ. Rev., 1, 26–37, 1993.

Plasil, J., Sejkora, J., Cejka, J., Skoda, R., and Golias, V.: Supergene mineralization of the Medvedin uranium deposit, Krkonose Mountains, Czech Republic, J. Geosci., 54, 15–56, 2009.

Prichard, H. M. and Brought, C.: Potential of ophiolite complexes to host PGE deposits, in: New Developments in Magmatic Ni-Cu and PGE Deposits, edited by: Li, C. and Ripley, E. M., 277–290, ISBN 9787116061187, https://orca.cardiff.ac.uk/id/eprint/12028 (last access: 3 July 2023), 2009.

Pushkarev, E. V., Ballhaus, C., Gottman, I., and Wirth, R.: The discovery of nano-cluster fabrics of PGM and natural platinum-rich gels; An alternative model of chromiteplatinum ore formation in Ural-Alaskan-type intrusions, 13th Internat. Platin. Symp., 30 June–6 July 2018, Ranch Hotel, Polokwane, South Africa, 158–159, 2018.

Ramdohr, P.: Rheingold als Seifenmineral, Jahreshefte des Geol. Landesamt Baden-württemb., 7, 87–95, 1965.

Reith, F., Stewart, L., and Wakelin, S. A.: Supergene gold transformation: Secondary and nano-particulate gold from southern New Zealand, Chem. Geol., 320/321, 32–45, https://doi.org/10.1016/j.chemgeo.2012.05.021, 2012.

Rivera, J., Reich, M., Schoenberg, R., González-jiménez, J. M., Barra, F., Aiglsperger, T., Proenza, J. A., and Carretier, S.: Platinum-group element and gold enrichment in soils monitored by chromium stable isotopes during weathering of ultramafic rocks, Chem. Geol., 499, 84–99, 2018.

Rosendorf, P., Vyskoč, P., Prchalová, H., and Fiala, D.: Estimated contribution of selected non-point pollution sources to the phosphorus and nitrogen loads in water bodies of the Vltava river basin, Soil Water Res., 11, 196–204, https://doi.org/10.17221/15/2015-SWR, 2016.

Rudashevsky, N. S., Garuti, G., Andersen, J. C., Kretser Yu, L., Rudashevsky, V. N., and Zaccarini, F.: Separation of accessoryminerals from rocks and ores by hydroseparation (HS) technology: method and application to CHR-2 chromitite, Niquelândia intrusion, Brazil, Trans.-Inst. Min. Metall. Sect. B, 111, B867–B894, 2002.

Sandmann, D. and Gutzmer, J.: Nature and distribution of PGE mineralisation in gabbroic rocks of the Lusatian Block, Saxony, Germany, Z. Dtsch. Ges. Geowiss., 166, 35–53, 2014.

Scholz, M., Stab, S., and Dziock, F.: Lebensräume der Elbe und ihrer Auen, Weißensee, Schweizerbart, ISBN-13: 978-3510653010, 2005.

Schulze, H., Bischoff, A., Palme, H., Spettel, B., Dreibus, G., and Otto, J.: Mineralogy and chemistry of Rumuruti: the first meteorite fall of the new R chondrite group, Meteoritics, 29, 275–286, https://doi.org/10.1111/j.1945-5100.1994.tb00681.x, 1994.

Shcheka, G. G., Lehmann, B., Gierth, E., Gömann, K., and Wallianos, A.: Macrocrystals of Pt-Fe alloy from the kondyor PGE placer deposit, Khabarovskiy Kray, Russia: Trace-element content, mineral inclusions and reaction assemblages, Can. Mineral., 42, 601–617, https://doi.org/10.2113/gscanmin.42.2.601, 2004.

Slingerland, R.: Role of hydraulic sorting in the origin of fluvial placers, J. Sediment. Res., 54, 137–150, 1984.

Stepanov, S. Y., Palamarchuk, R. S., Kozlov, A. V., Khanin, D. A., Varlamov, D. A., and Kiseleva, D. V.: Platinum-group minerals of Pt-placer deposits associated with the svetloborsky Ural-Alaskan type massif, middle urals, Russia, Minerals, 9, 1–25, https://doi.org/10.3390/min9020077, 2019.

Suh, C. E. and Lehmann, B.: Morphology and electron-probe microanalysis of residual gold-grains at Dimako, Southeast Cameroon, Neues Jahrb. Mineral.-Monatshefte, 2003, 6, 255–275, https://doi.org/10.1127/0028-3649/2003/2003-0255, 2003.

Sysalová, J., Kučera, J., Drtinová, B., Červenka, R., Zvěřina, O., Komárek, J., and Kameník, J.: Mercury species in formerly contaminated soils and released soil gases, Sci. Total Environ., 584/585, 1032–1039, 2017.

Tolstykh, N., Foley, J. Y., Sidorov, E. G., and Laajoki, K. V.: Composition of the platinum-group minerals in the Salmon River placer deposit, Goodnews Bay, Alaska, Can. Mineral., 40, 463–471, 2002a.

Tolstykh, N., Krivenko, A., Sidorov, E., Laajoki, K., and Podlipsky, M.: Ore mineralogy of PGM placers in Siberia and the Russian Far East, Ore Geol. Rev., 20, 1–25, 2002b.

Tolstykh, N., Sidorov, E., and Kozlov, A.: Platinum-group minerals from the Olkhovaya-1 placers related to the Karaginsky ophiolite complex, Kamchatskiy Mys peninsula, Russia, Can. Mineral., 47, 1057–1074, https://doi.org/10.3749/canmin.47.5.1057, 2009.

Tolstykh, N. D., Sidorov, E. G., and Kozlov, A. P.: Platinum-group minerals in lode and placer deposits associated with the ural-alaskan-type Gal'moenan complex, Koryak-Kamchatka Platinum Belt, Russia, Can. Mineral., 42, 619–630, https://doi.org/10.2113/gscanmin.42.2.619, 2004.

Tolstykh, N. D., Sidorov, E. G., and Krivenko, A. P.: Platinum-group element placers associated with Ural-Alaskan type complexes, in: Exploration for deposits of platinum-group elements, Mineralogical Association of Canada, Short Course Series, Vol. 35, edited by: Mungall, J. E., 113–143, ISBN: 0-921294-35-2, 2005.

Tredoux, M., Lindsay, J. M., Davies, G., and McDonald, I.: The fractionation of platinum-group elements in magmatic systems,

with the suggestion of a novel causal mechanism, South Afr. J. Geol., 98, 157–167, 1995.

Velebil, D. and Zacharias, J.: Fluid inclusion study of the Horní Luby cinnabar deposit, Saxothuringian Zone, Bohemian Massif: clues for the metamorphic remobilization of mercury, J. Geosci., 58, 283–298, https://doi.org/10.3190/jgeosci.145, 2013.

Vink, R. J., Behrendt, H., and Salomons, W.: Point and diffuse source analysis of heavy metals in the Elbe drainage area: Comparing heavy metal emissions with transported river loads, Hydrobiologia, 410, 307–314, 1999.

Vital, H., Stattegger, K., and Garbe-Schoenberg, C.-D.: Composition and trace-element geochemistry of detrital clay and heavy-mineral suites of the lowermost Amazon River; a provenance study, J. Sediment. Res., 69, 563–575, 1999.

Wagner, P. A.: The Platinum Deposits and Mines of South Africa, Edingburgh, Oliver and Boyd, ISBN: 0869770233, 1929.

Walter, R.: Geologie von Mitteleuropa, Schweizerbart'sche Verlagsbuchhandlung, Stuttgart, Schweizerbart, ISBN: 3510651499, 1995.

Weiser, T. W.: Platinum-group minerals (PGM) in placer depos-its, in: The Geology, Geochemistry, Mineralogy and Mineral Beneficiation of Platinum-Group Elements, edited by: Cabri, L. J., 721–756, Canadian Institute of Mining, Metallurgy and Petroleum, Montreal, ISBN: 9781894475273, 2002.

Weiser, T. W. and Bachmann, H. G.: Platinum-group minerals from the Aikora River area, Papua New Guinea, Can. Mineral., 37, 1131–1145, 1999.

Wierchowiec, J.: Placer gold and other economic minerals from the remnants of palaeofan deposits in the foreland of the East Sudetes, Poland, Acta Geol. Pol., 57, 523–537, 2007.

Wirth, R., Reid, D., and Schreiber, A.: Nanometer-sized platinum-group minerals (PGM) in base metal sulfides: New evidence for an orthomagmatic origin of the merensky reef pge ore deposit, bushveld complex, South Africa, Can. Mineral., 51, 134–155, https://doi.org/10.3749/canmin.51.1.143, 2013.

Yesares, L., Sáez, R., Nieto, J. M., de Almodóvar, G. R., and Cooper, S.: Supergene enrichment of precious metals by natural amalgamation in the Las Cruces weathering profile (Iberian Pyrite Belt, SW Spain), Ore Geol. Rev., 58, 14–26, 2014.

Zaccarini, F., Proenza, J. A., Ortega-Gutiérrez, F., and Garuti, G.: Platinum group minerals in ophiolitic chromitites from Tehuitzingo (Acatlán complex, southern Mexico): Implications for post-magmatic modification, Mineral. Petrol., 84, 147–168, https://doi.org/10.1007/s00710-005-0075-7, 2005.

Zaccarini, F., Pushkarev, E., Garuti, G., Krause, J., Dvornik, J. P., Stanley, C., and Bindi, L.: Platinum-group minerals (PGM) nuggets from alluvial-eluvial placer deposits in the concentrically zoned mafic-ultramafic Uktus complex (Central Urals, Russia), Eur. J. Mineral., 25, 519–531, 2013.

Zaccarini, F., Garuti, G., Pushkarev, E., and Thalhammer, O.: Origin of Platinum Group Minerals (PGM) inclusions in chromite deposits of the urals, Minerals, 8, 1–21, https://doi.org/10.3390/min8090379, 2018.

Zaccarini, F., Economou-Eliopoulos, M., Kiseleva, O., Garuti, G., Tsikouras, B., Pushkarev, E., and Idrus, A.: Platinum Group Elements (PGE) Geochemistry and Mineralogy of Low Economic Potential (Rh-Pt-Pd)-Rich Chromitites from Ophiolite Complexes, Minerals, 12, 1565, https://doi.org/10.3390/min12121565, 2022.

Zachariáš, J.: Structural evolution of the Mokrsko-West, Mokrsko-East and Čelina gold deposits, Bohemian Massif, Czech Republic: Role of fluid overpressure, Ore Geol. Rev., 74, 170–195, 2016.

Zachariáš, J., Morávek, P., Gadas, P., and Pertoldová, J.: The Mokrsko-West gold deposit, Bohemian Massif, Czech Republic: Mineralogy, deposit setting and classification, Ore Geol. Rev., 58, 238–263, 2014.

Zieger, J., Bittner, L., Gärtner, A., Hofmann, M., Gerdes, A., Marko, L., and Linnemann, U.: U–Pb ages of magmatic and detrital zircon of the Döhlen Basin: geological history of a Permian strike-slip basin in the Elbe Zone (Germany), Int. J. Earth Sci., 108, 887–910, 2019.